[redacted]

UMRL
040

UNIVERSITY OF MICHIGAN

CONFIDENTIAL

Cat 4
~~Cat-4~~
Decl 12/80

AUG 1 1971
JUL 5 1972
MAY 10 1973
JUL 16 1974
DEC 1974

2476-1-F
18 April 1956

2476-1-F = RL-2053

Final Report on

ANALYSIS OF PADAR AND ITS MODIFICATIONS

T. B. Curtz, M. L. Barasch, H. Brysk,
T. A. Kaplan, R. E. Kleinman,
W. C. Orthwein, and H. Weil

Purchase Order 130-35 under
Air Force Contract AF 33(616)-3186

"NATIONAL SECURITY INFORMATION"

"Unauthorized Disclosure Subject to Criminal Sanctions".

[redacted]

THE UNIVERSITY OF MICHIGAN
Engineering Research Institute
Willow Run Laboratories
Ypsilanti, Michigan

DOWNGRADED AT 12 YEAR INTERVALS; NOT AUTOMATICALLY DECLASSIFIED. DOD DIR 5200.10

CONFIDENTIAL

[redacted]

TABLE OF CONTENTS

NOMENCLATURE

G = antenna gain

M = missile position

N = point of reflection on earth, "bounce point"

O = center of earth

P = PADAR receiver position

P_1 = peak transmitted power

P_2 = minimum detectable received power

R = radius of earth

T = transmitter position

c = velocity of light

h = true height of PADAR receiver

h_1 = height of PADAR receiver (flat earth)

h_2 = height of transmitter (flat earth)

h' = height of PADAR receiver minus height of transmitter

ℓ_1 = distance from PADAR receiver, P, to "bounce point", N

ℓ_2 = distance from transmitter, T, to "bounce point", N

r = distance from transmitter, T, to PADAR receiver, P

$u = \frac{\ell}{r}$

$v = 1 - \cos \phi$

α = angle between $\overline{PN}$ and the normal to $\overline{PO}$ measured positive counterclockwise

α_1 = angle between the horizontal (at the "bounce point") and the ray to the PADAR receiver

α_2 = angle between the horizontal (at the "bounce point") and the ray to the transmitter

Declassified IAW E.O. 11652 dated 8March72
Section 5, paragraph D

β = angle from h (height of PADAR) to r (transmitter-receiver direction), measured positive clockwise

γ = angle between ℓ_1 (receiver-reflector direction) and ℓ_2 (transmitter-reflector direction)

δ = $c\Delta t$ = path length difference between direct and reflected paths

ε = a higher order error term in Taylor series for range error

θ = angle from horizontal (at receiver) to transmitter direction measured positive counterclockwise

θ_1 = angle between the horizontal at the "bounce point" and r (transmitter-receiver direction) measured positive counter-clockwise

λ = wavelength

σ = radar cross-section

ϕ = angle between r (transmitter-receiver direction) and ℓ_1 (receiver-"bounce point" direction)

ψ = angle measured from the earth's radius at the "bounce point" to $\overline{PO}$, measured positive counterclockwise

ω = angle from $\overline{PO}$, normal to earth from PADAR receiver, to ℓ_1 (receiver-"bounce point" direction), measured positive counterclockwise

$[\xi,\zeta]$ = angular coordinates of transmitter for cross-section calculations-defined in Appendix 1. The remaining notation used in the Appendix is entirely contained therein and is defined when used.

Δt = time difference required for energy to travel from transmitter to receiver over two different paths

Δx_i = error in x_i where x_i is a measured variable, e.g., θ, h_1, . . .

$\sigma_{\Delta x_i}$ = standard deviation of error in x_i

ANALYSIS OF PADAR AND ITS MODIFICATIONS

Introduction

PADAR came into existence as the result of Fairchild's effort to fulfill the need in fighter-fighter and fighter-bomber duels for the U. S. aircraft to obtain range information about the enemy at greater distances. Their idea is based on the comparison of a direct and a reflected path*.

In Appendix 2 the following considerations for this range finding system will be analyzed: general slope and roughness of the terrain, the curvature of the earth, propagation effects and measurement errors. As discussed below, some modifications toward greater complexity of the system are necessary for successful ranging under operational conditions; limitations remain.

It has been suggested that bombers might use a method based on the Fairchild idea for defense against missiles of the beam-rider type. The University of Michigan was asked to examine this possibility under the assumption that the enemy defensive system would be similar to Talos. The results of Appendix 3 show that in principle this modification of PADAR will usually give accurate passive range information at greater distances than active radar could obtain if both signals are detectable. It is strongly recommended that study of the application of PADAR to the bomber defense problem be continued.

---

*Fairchild's development of this idea is discussed in References 1 to 5.

We do not recommend immediate implementation, because of the following points:

(a) When the missile is on the transmitter-PADAR line of sight, no range determination can be made by PADAR methods.

(b) We lack radar cross-sections of enemy missiles. (The bistatic cross-section needed is at least 1 to 10 square feet for typical interception trajectories. It is likely that all enemy missiles will have cross-sections of this order of magnitude; however, a few calculations should be done to verify this.)

(c) An analysis of enemy radar patterns is required to determine whether sufficient side lobe energy will exist to permit PADAR ranging.

(d) We do not know whether there is actually a tactical advantage in the use of PADAR over presently conceived active radar defense systems against beam-rider missiles.

An experimental check of some of the concepts involved has been suggested by WADC, using two F-86D aircraft and the present Fairchild PADAR equipment. The very poor accuracy to be expected in such an experiment and the probability of detecting the reflecting F-86D are discussed in Appendix 3. We do not recommend that this experiment be performed. The F-86D cross-sections used in this discussion are given in Appendix 1.

Ranging Capabilities of PADAR

1. PADAR, as presently described in the Fairchild reports and using the equations given therein, is capable of successful ranging provided:
   a) The ranges are fairly short (of the order of 80 miles).
   b) The terrain at the specular reflection point does not have large scale irregularities.
   c) The terrain has an average slope which is perpendicular to the earth's radius.
   d) Sufficient data smoothing is used.

2. The limitation to short ranges can be removed by inserting the data in the equations of Appendix 2 (2.3.1) which take the curvature of the earth into account exactly.

3. Limitation 1.c) and, in some instances, limitation 1.b) can be removed if, in addition to the measurements proposed for PADAR, the angle between the horizontal plane at the PADAR and the ray from the specular reflection point to the PADAR is measured. The data are then to be used in the equations of Appendix 2 (2.5).

4. Over very rugged or heavily built up terrain, PADAR should not be expected to give usable range data.

5. Optimum conditions for application of PADAR to detecting and ranging on airborne reflectors occur when the angle between the reflector-PADAR direction and the transmitter-PADAR direction is large, and if the altitude difference between the PADAR plane and the transmitter is a maximum.

To obtain range against an airborne reflecting target it is necessary to measure an additional angle over PADAR.

Declassified IAW E.O. 11652 dated 8March72
Section 5, paragraph D

Tactical Considerations

The purpose of this investigation has been consideration of problems relating to the feasibility of determining range by PADAR in certain given situations. Range information on enemy aircraft or missiles is clearly always potentially useful. At the same time, a number of important questions concerning the tactical use of PADAR range information naturally suggest themselves. Although no effort will be made here to answer these questions, their statement may prove helpful in evaluating the usefulness of PADAR.

1) Passive detection can work at ranges considerably beyond the detection range of ordinary airborne radar. With PADAR, passive range information may also be obtained with the accuracies indicated below. This presupposes, however, that the enemy has a pulsed transmitter operating; one must examine under what circumstances this will be true.

2) If the detection range of the enemy radar can be estimated with reasonable accuracy, passive range information can be used until the PADAR aircraft is known to be detected. After this, is there any advantage in using PADAR rather than a more accurate active radar?

3) Is the additional information worth the possible weight, space, and cost penalties?

4) In the beam-rider missile case, the missile will presumably be launched at ranges short enough to preclude evasive action by the bomber. Can successful countermeasures be taken at ranges greater than those attained by active radar? If the answer to this question is "no", do other possible advantages of remaining passive outweigh the greater accuracy attainable in active operation?

Declassified IAW E.O. 11652 dated 8March72
Section 5, paragraph D

APPENDIX 1

BISTATIC RADAR CROSS-SECTIONS OF THE F-86D AT X-BAND

1.1 The Cross-Sections Required

One of the problems specified in this contract was the determination of some of the bistatic cross-section values of the F-86D. This information is employed in the analysis of the proposed experiment described in Appendix 3 (3.3). In this Appendix we shall discuss the derivation of these cross-sections, and present the results obtained.

A bistatic radar cross-section is defined as one for which the transmitter and receiver are not coincident. In this problem, the receiver is nose-on to the F-86D, while the direction to the transmitter lies on one of a set of cones about the rear of the plane. These cones have half-angles from 20° to 60°, varying by 10° steps. Further, horizontal polarization is specified for both transmitter and receiver, that is, the transmitted $\hat{E}$ vector is parallel to the plane of the wings, and the receiving antenna accepts only this polarization. Finally, an X-band frequency of 9400 Mc, or wavelength of 0.105 feet was used.

For a comparison with experiment of theoretical results obtained by the method employed, see Reference 6. A full discussion of geometric and physical optics methods is also given in Reference 6.

1.2 Break-up of Plane

As a first step in obtaining the cross-sections, the airplane is simulated by a set of components of simple geometric shapes, whose dimensions and orientations are recorded. A random phase argument enables us to

treat these components as independent scatterers. Their separate cross-sections are therefore obtained and added, taking shadowing into account. We now present the break-up which was used.

The wings were considered as truncated elliptic cones having dimensions as shown in Figure 1.2-1

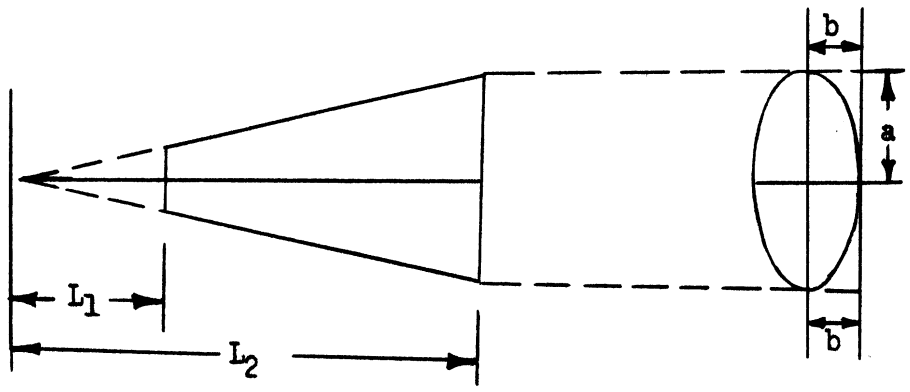

Figure 1.2-1

$$L_1 = 255'', \; L_2 = 470'', \; a = 46'', \; \eta = a/b = 6$$

and a sweepback angle $\sigma = 35^\circ$. Angle of attack and dihedral were taken as zero.

The horizontal and vertical tail surfaces, like the wings, were modeled by truncated elliptic cones. The dimensions are:

(a) Horizontal tail surfaces

$L_1 = 80"$, $L_2 = 160"$, $a = 19"$, $\eta = 6$

and a sweepback angle $\Lambda = 28^\circ$

(b) Vertical tail surface

$L_1 = 55"$, $L_2 = 150"$, $a = 31"$, $\eta = 7$

and a setback angle from the vertical of $\Lambda = 35^\circ$

The nose of the fuselage was treated as a prolate spheroid and an elliptic cylinder combined as indicated in Figure 1.2-2.

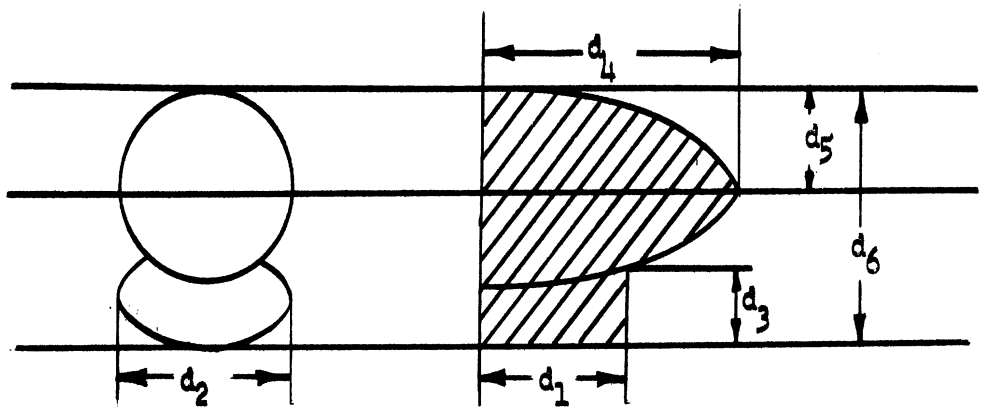

Figure 1.2-2

Here,

$d_1 = 49"$, $d_2 = 48"$, $d_3 = 20"$, $d_4 = 89"$, $d_5 = 24"$, $d_6 = 62"$.

The midsection of the fuselage, measured from the front end of the canopy to the point at which the trailing edge of the wing joins the fuselage, was considered the exposed surface of two intersecting elliptic cylinders, as in Figure 1.2-3.

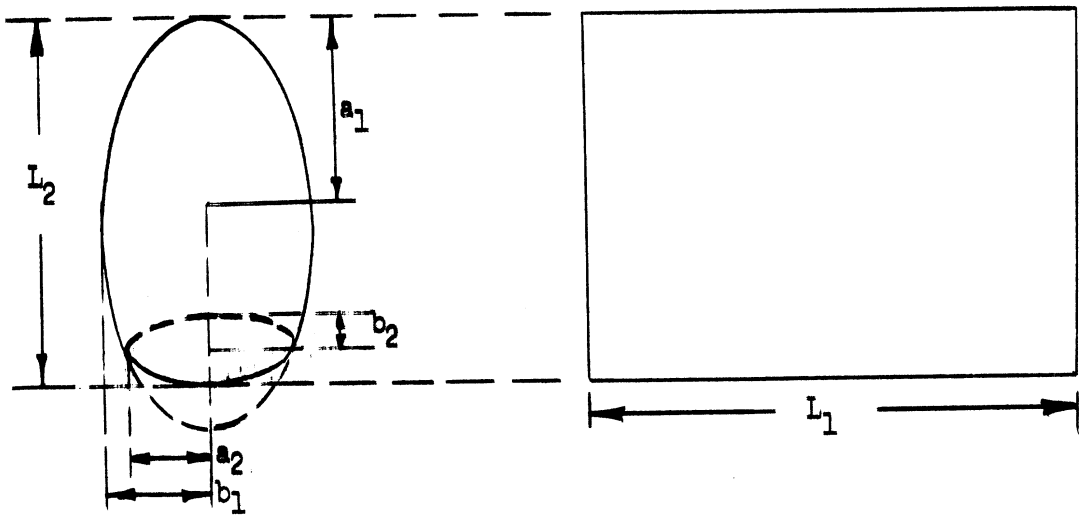

Figure 1.2-3

For this component

$$a_1 = 48", \; b_1 = 29", \; a_2 = 27.5", \; b_2 = 5.5", \; L_1 = 180", \; L_2 = 68.5".$$

Only the front half of the wing tanks contributes. These were modeled by prolate spheroids whose dimensions are (see Fig. 1.2-4):

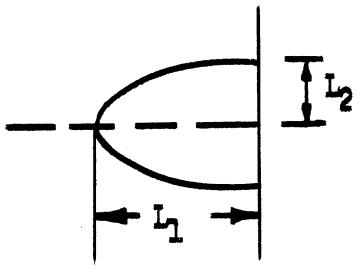

$L_1 = 51", \; L_2 = 12"$

Figure 1.2-4

All dimensions were obtained from the configuration drawing contained in "Standard Aircraft Characteristics", Wright Air Development Center, 3 August 1951. This drawing was neither large nor detailed, so that we were forced to estimate certain dimensions not explicitly given.

1.3 Shadowing

The cross-section formulas to be employed are all either of physical or geometric optics type. In the former case, it is the dimensions of the illuminated area of the component which appear in the expressions, while in the latter, a contribution to the cross-section is obtained only if the so-called "stationary-phase point" is illuminated. Therefore it was necessary to determine how components shadow others as a function of transmitter aspect.

1.4 Cross-Section Formulas

The prolate spheroid cross-section was obtained from the expression

$$\sigma = \pi a^2 \left[\frac{(\cos\theta_R+\cos\theta_T)^2+(\sin\theta_R\sin\phi_R+\sin\theta_T\sin\phi_T)^2+(\sin\theta_R\cos\phi_R+\sin\theta_T\cos\phi_T)^2}{(\cos\theta_R+\cos\theta_T)^2+(\sin\theta_R\sin\phi_R+\sin\theta_T\sin\phi_T)^2+\eta^2(\sin\theta_R\cos\phi_R+\sin\theta_T\cos\phi_T)^2} \right]^2$$

Here a is the semi-major axis, b the semi-minor axis, and $\eta = a/b$. θ and ϕ are the usual spherical coordinates of the vectors to the transmitter (T) and receiver (R), as illustrated in Figure 1.5-1. The Z-axis is taken vertical; the X-axis points forward through the nose of the plane. We are

therefore interested only in the case $\theta_R = \pi/2$, $\phi_R = 0$. The spheroid is assumed horizontal, with its nose pointing forward.

This is a geometric optics formula. That is, it is equal to $\pi R_1 R_2$, where R_1 and R_2 are the principal radii of curvature at the specular reflection point corresponding to a choice of transmitter and receiver aspect. Such an expression is valid for short wavelengths such as we have here. It is independent of transmitter and receiver polarizations. The contribution it yields should be used only when the specular point is not shadowed.

For the elliptic cylinders, physical optics cross-sections, which are polarization-dependent, were employed. The expressions are:

For the lower middle fuselage and the lower front of the fuselage

$$\sigma(H,H) = \frac{4\lambda \cos^4 \theta_T \cos^2 \phi_T \, a^2 b^2}{\pi \left[a^2 \sin^2 \theta_T \sin^2 \phi_T + b^2 \cos^2 \theta_T\right]^{3/2}} \frac{\sin^2 \frac{kDL}{2}}{D^2} ,$$

where $D = 1+\sin\theta_T \cos\phi_T$, a = semi-major axis, b = semi-minor axis, and L = length of the cylinder, λ = wavelength and $k = 2\pi/\lambda$. θ_T and ϕ_T are the usual aspect angles. $\theta_R = \pi/2$ and $\phi_R = 0$ have been inserted explicitly.

For the upper middle fuselage, which is rotated through $\pi/2$ about its axis from the orientation of the others, a and b are interchanged in the expression, so that

$$\sigma(H,H) = \frac{4\lambda \cos^4 \theta_T \cos^2 \phi_T \, a^2 b^2}{\pi \left[a^2 \cos^2 \theta_T + b^2 \sin^2 \theta_T \sin^2 \phi_T\right]^{3/2}} \frac{\sin^2 \frac{kDL}{2}}{D^2} .$$

$\frac{kL}{2}$ is very large, being of the order of 200π to 400π. Therefore, any slight error in specifying the aspect, which corresponds to a small uncertainty in D, may change the argument of $\sin^2 \frac{kDL}{2}$ significantly.

Our procedure is then to average the $\sin^2 \frac{kDL}{2}$ to 1/2, yielding a cross-section value, which, assuming the validity of the magnitude predicted by physical optics, would be approached by the average value of a large number of observations "at" each aspect considered.

For the wings and tail surfaces, which we represent by truncated elliptic cones, we use again a physical optics formula in which an averaging has likewise been performed.

For the starboard wing and starboard horizontal tail,

$$\sigma(H,H) = \frac{2\eta^2 (L_1+L_2)\tan\beta \left\{ [\hat{n}_o \cdot \hat{a}][\vec{N} \cdot \hat{d}] - [\hat{n}_o \cdot \vec{N}][\hat{a} \cdot \hat{d}] \right\}^2}{k(A^2+\eta^2 B^2)^{3/2} \left(\tan\beta \sqrt{A^2 + \eta^2 B^2} + C\right)^2} ,$$

wherein $k = \frac{2\pi}{\lambda}$,

L_1 and L_2 are the two truncation lengths, measured from the vertex of the cone,

$\tan\beta = \frac{b}{L_2}$ and $\tan\alpha = \frac{a}{L_2}$, where b and a are the semi-minor and semi-major axes of the ellipse at L_2,

$\eta = \tan\alpha / \tan\beta$

$$A = \cos\theta_R + \cos\theta_T ,$$

$$B = \sin\theta_R \cos(\phi_R + \delta) + \sin\theta_T \cos(\phi_T + \delta) ,$$

$$C = \sin\theta_R \sin(\phi_R + \delta) + \sin\theta_T \sin(\phi_T + \delta),$$

δ is the sweepback angle from broadside,

$$\hat{n}_o = \hat{X}\cos\theta_R + \hat{Y}\sin\theta_R\cos(\phi_R + \delta) + \hat{Z}\sin\theta_R\sin(\phi_R + \delta),$$

$$\hat{a} = -\sin\theta_T\,\hat{X} + \hat{Y}\cos\theta_T\cos(\phi_T + \delta) + \hat{Z}\cos\theta_T\sin(\phi_T + \delta) ,$$

$$\hat{d} = -\sin\theta_R\,\hat{X} + \hat{Y}\cos\theta_R\cos(\phi_R + \delta) + \hat{Z}\cos\theta_R\sin(\phi_R + \delta),$$

$$\vec{N} = \hat{X}A + \hat{Y}B - \hat{Z}\tan\beta\sqrt{A^2 + \eta^2 B^2}.$$

For the port wing and port horizontal tail, δ is replaced by $\pi - \delta$ everywhere in this expression.

For the vertical tail, we use the same form with the following replacements:

$$A = \sin\theta_T \sin\phi_T + \sin\theta_R \sin\phi_R ,$$

$$B = (\cos\theta_R + \cos\theta_T)\sin\delta + (\sin\theta_R\cos\phi_R + \sin\theta_T\cos\phi_T)\cos\delta ,$$

$$C = (\cos\theta_R + \cos\theta_T)\cos\delta - (\sin\theta_R\cos\phi_R + \sin\theta_T\cos\phi_T)\sin\delta ,$$

δ is the sweepback from the vertical ,

$$\hat{n}_o = \hat{X}\sin\theta_R\sin\phi_R + \hat{Y}\left[\cos\theta_R\sin\delta + \sin\theta_R\cos\phi_R\cos\delta\right] + \hat{Z}\left[\cos\theta_R\cos\delta - \sin\theta_R\cos\phi_R\sin\delta\right] ,$$

$$\hat{a} = \hat{X}\cos\theta_T\sin\phi_T - \hat{Y}\left[\sin\theta_T\sin\delta - \cos\theta_T\cos\phi_T\cos\delta\right] - \hat{Z}\left[\sin\theta_T\cos\delta + \cos\theta_T\cos\phi_T\sin\delta\right],$$

$$\hat{d} = \hat{X}\cos\theta_R\sin\phi_R - \hat{Y}\left[\sin\theta_R\sin\delta - \cos\theta_R\cos\phi_R\cos\delta\right] - \hat{Z}\left[\sin\theta_R\cos\delta + \cos\theta_R\cos\phi_R\sin\delta\right],$$

The stationary phase evaluation which yields these elliptic cone cross-section expressions was found to be valid for $\delta \geq 20^\circ$ although it is not valid further back.

Finally, the shadowing procedure used for elliptic cone surfaces will be explained. The physical optics formulation used prescribes an integration over the illuminated surface only. The contribution to the cross-section depends explicitly upon the limit of integration corresponding to the edge of the shadow. However, the surface currents at the shadow boundary really go continuously to zero, and do not, therefore, contribute to the cross-section like the currents at the tip of a body.

For this reason we have treated the factor $L_1 + L_2$ in the following way, which should be a satisfactory approximation:

1. If both ends of the body are illuminated, we use the full value $L_1 + L_2$.
2. If one end is shadowed, only the L corresponding to the other end is used.
3. If both ends are shadowed, the contribution to the cross-section is negligible.

1.5 Results

In this section curves for $\sigma(H,H)$ of the F-86D are given in Figure 1.5-2 through 1.5-6. The cross-section in square feet is plotted as a function of ξ (the rotation angle around the cone) for fixed values of ζ, the cone half-angle. The definition of these angles may be clarified by the following sketch.

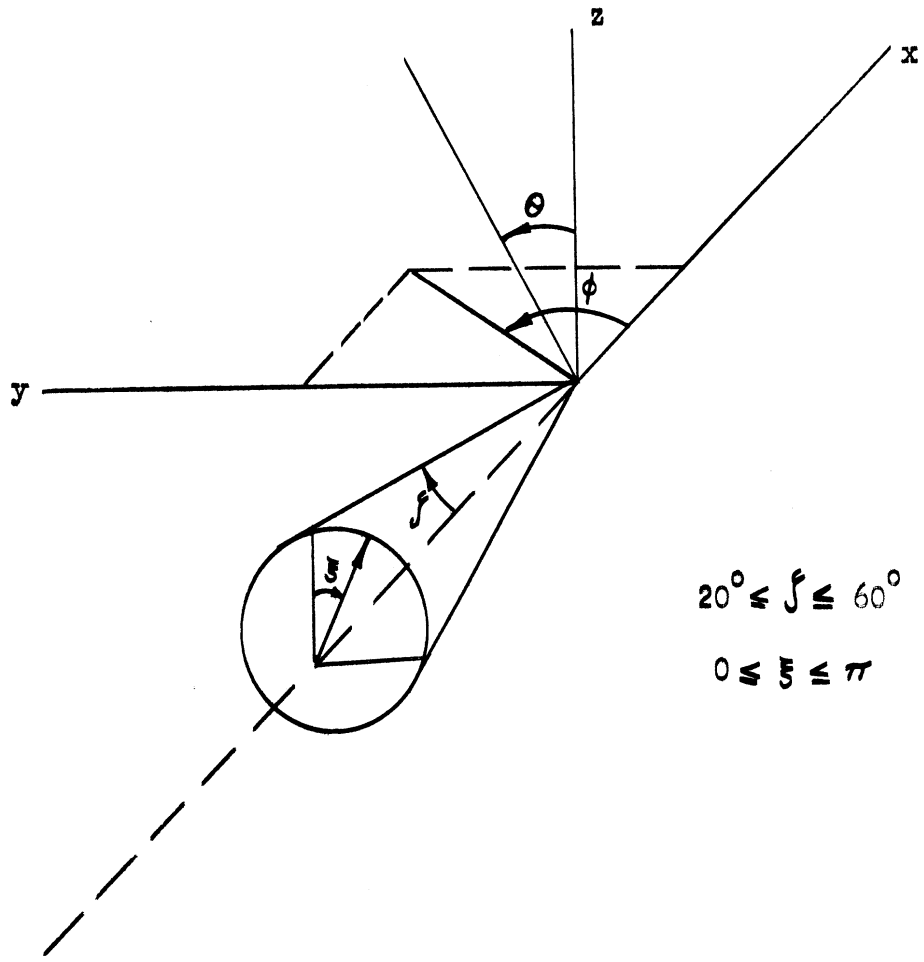

Figure 1.5-1

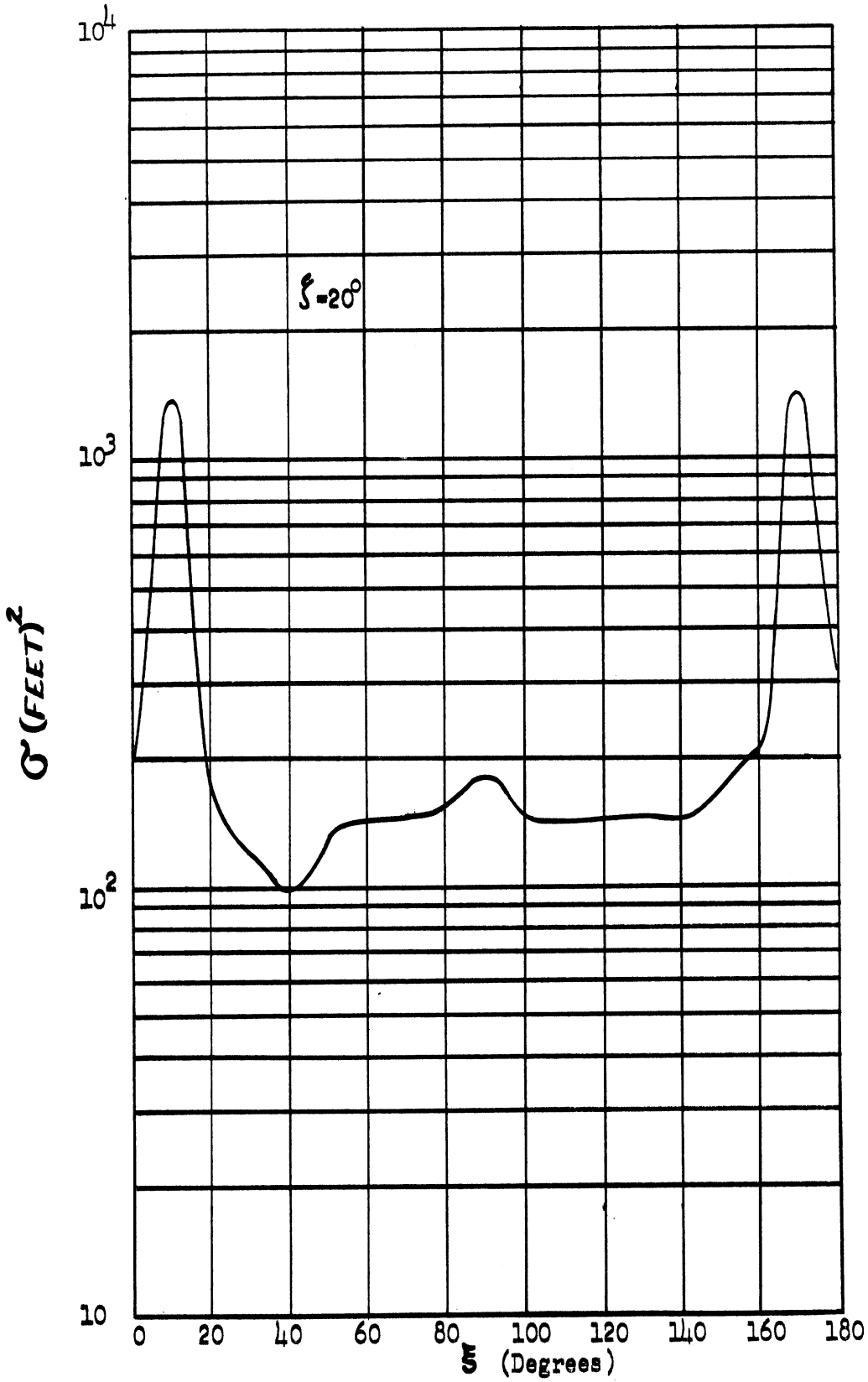

Figure 1.5-2

Bistatic cross-section of the F86-D, as a function of position on the "transmitter cone" for receiver nose-on.

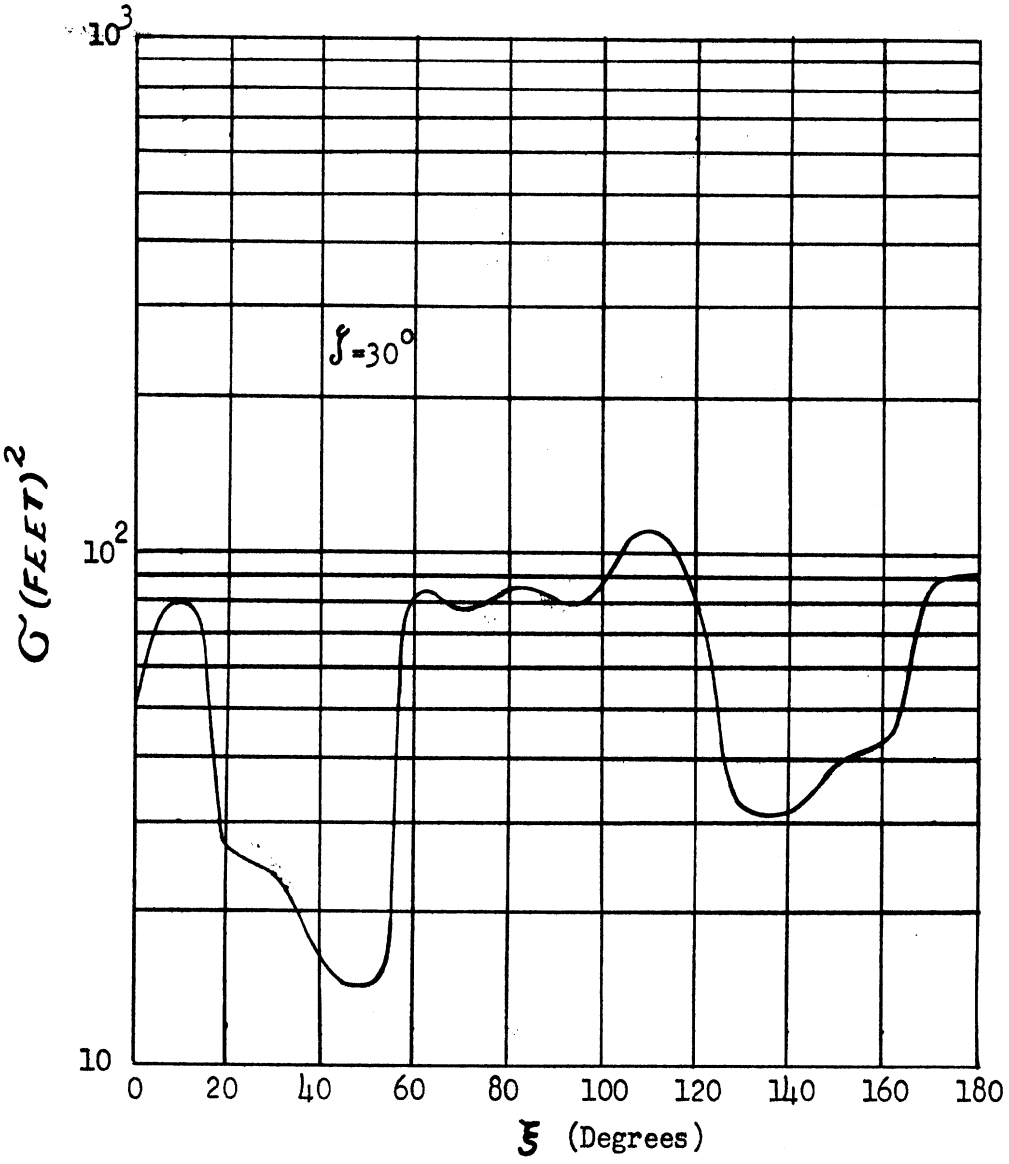

Figure 1.5-3
Bistatic cross-section of the F86-D, as a function of position on the "transmitter cone" for receiver nose-on.

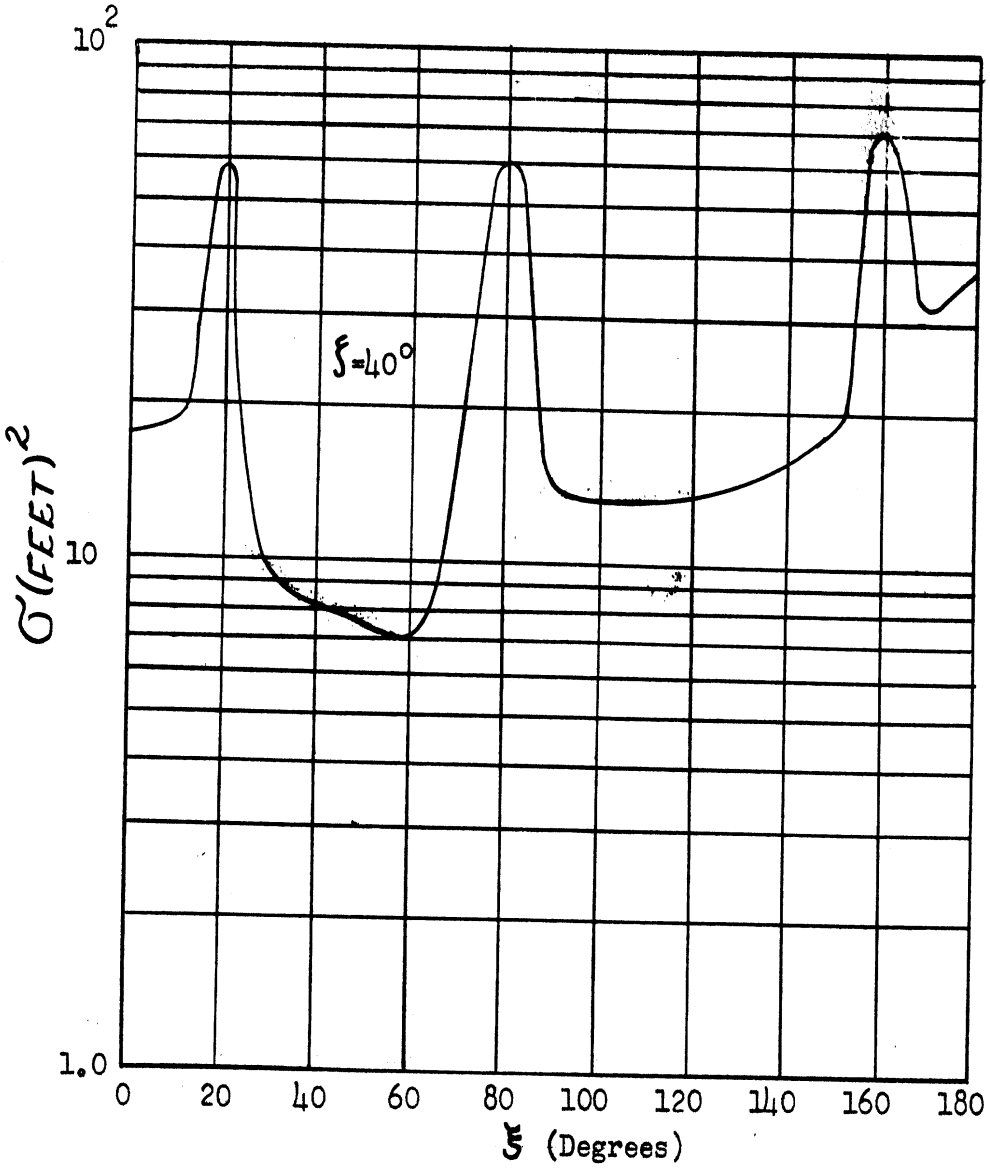

Figure 1.5-4

Bistatic cross-section of the F86-D, as a function of position on the "transmitter cone" for receiver nose-on.

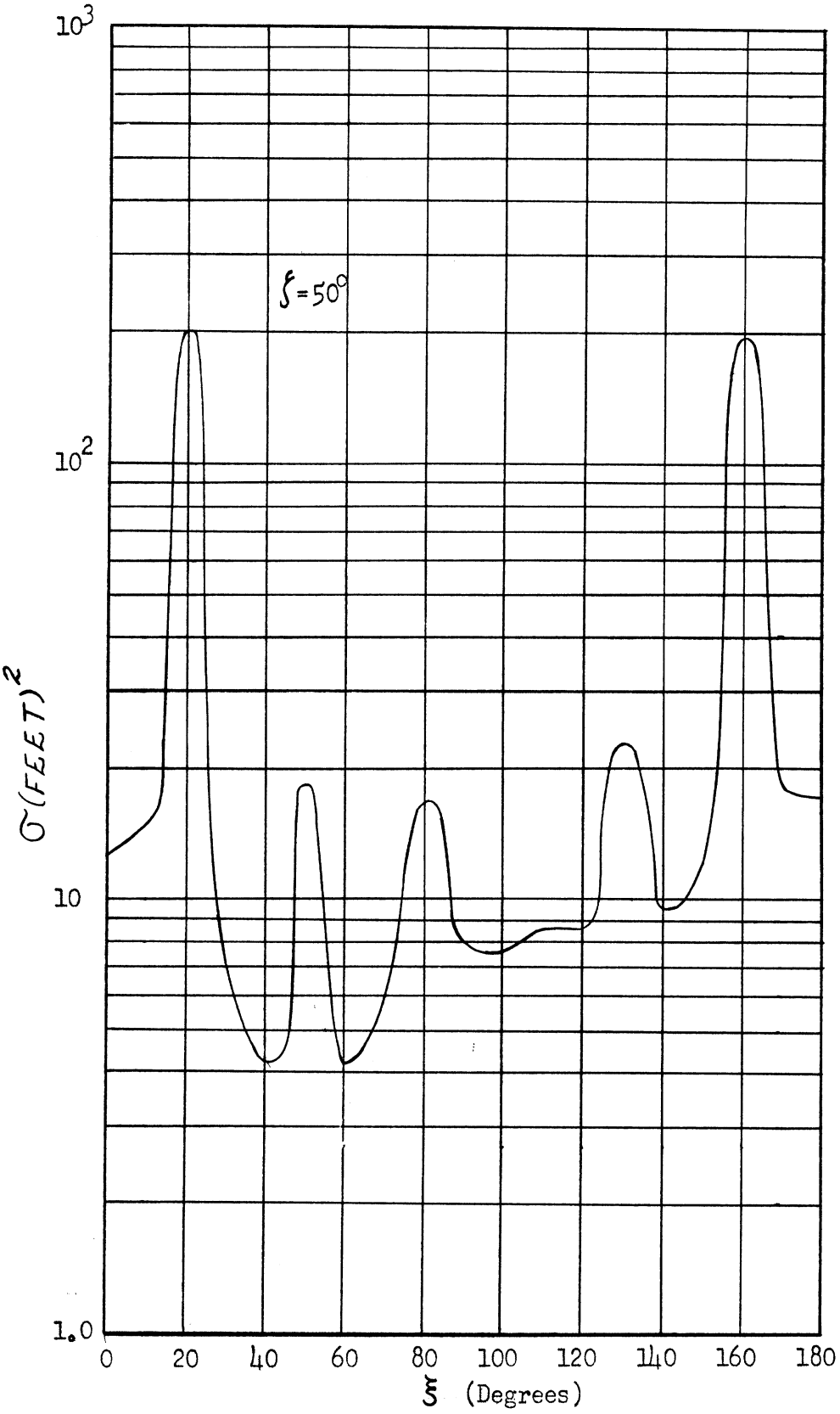

Figure 1.5-5

Bistatic cross-section of the F86-D, as a function of position on the "transmitter cone" for receiver nose-on.

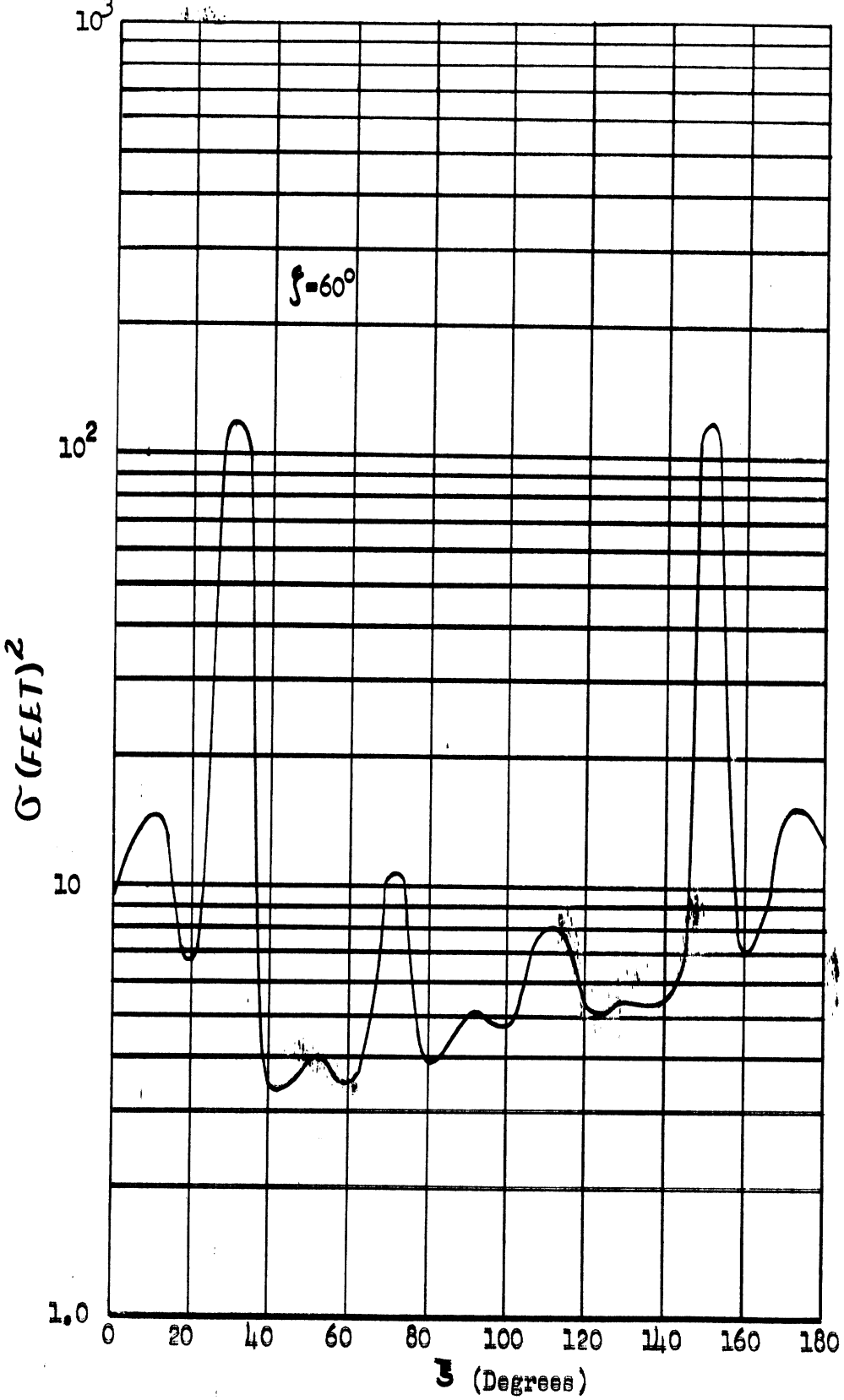

Figure 1.5-6

Bistatic cross-section of the F86-D, as a function of position on the "transmitter cone" for receiver nose-on.

APPENDIX 2

BASIC CONSIDERATIONS RELATING TO PADAR

2.1 Preliminary Results and PADAR Equations

Fairchild's present experimental set-up differs from PADAR as described in References 1 through 4 in that the target elevation angle is not measured and the target plane flies at a known altitude. Figure 2.1-1, which is reproduced from Reference 5, shows a typical A-scope presentation photographed during one of the first runs. The sharp, nearly vertical, leading edge of the pulse makes possible accurate reading of the time delay. The available data show that the errors in range presently being obtained can be tolerated. It will be observed that the experiments do not involve the angular measurement which would actually be required in practice. However, the analysis of ranging error shows that as range increases so does the importance of error in the angle measurement, and it will eventually be the dominant source of error for ranges that should be of interest.

Figure 2.1-1

The analysis of ranging error also shows that the range accuracy attainable at long ranges can be greatly improved by adequate consideration of the curvature of the earth.

To determine the PADAR range equation consider Figure 2.1-2. P represents the PADAR receiver and T the transmitter, whose existence and range is to be determined. The dotted line is parallel to the ground and the reflection is assumed to be specular ($\alpha_1 = \alpha_2$).

Once T is detected, the information measured by the PADAR is θ_1, h_1, and

$$\Delta t = (\ell_1 + \ell_2 - r)/c,$$

where c is the velocity of light.

To obtain r from this data note that

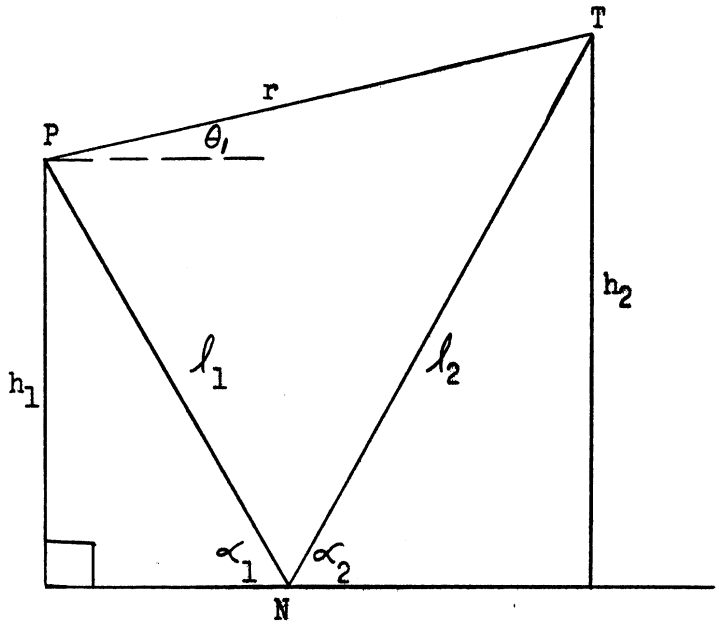

Figure 2.1-2

$$\ell_1 = \frac{h_1}{\sin\alpha_1}, \quad \ell_2 = \frac{h_1 + r \sin\theta_1}{\sin\alpha_1}, \tag{2.1.1}$$

$$\delta = c\Delta t = \ell_1 + \ell_2 - r = \frac{h_1}{\sin\alpha_1} + \frac{h_1 + r \sin\theta_1}{\sin\alpha_1} - r, \tag{2.1.2}$$

$$r \cos\theta_1 = \frac{h_1}{\tan\alpha_1} + \frac{h_1 + r \sin\theta_1}{\tan\alpha_1} . \tag{2.1.3}$$

From (2.1.2) and (2.1.3) we get

$$r = \frac{\delta \cos\alpha_1}{(\cos\theta_1 - \cos\alpha_1)} \tag{2.1.4}$$

which may be converted to the form used by Fairchild, namely

$$r = \frac{2\, h_1(h_1 + r \sin\theta_1)}{\delta} - \frac{\delta}{2} . \tag{2.1.5}$$

2.2 Accuracy of Range Determinations

In the measurement of h_1, δ, and θ_1 there are unavoidable errors. Their effect may be expressed by the first order terms of a Taylor expansion of r, namely

$$\Delta r = \frac{\partial r}{\partial \theta_1} \Delta\theta_1 + \frac{\partial r}{\partial h_1} \Delta h_1 + \frac{\partial r}{\partial \delta} \Delta\delta \tag{2.2.1}$$

provided the remainder is negligible. Here Δr is the error in r due to errors in θ_1, δ, and h_1. If $\Delta\delta$, $\Delta\theta_1$, and Δh_1 are considered to be random errors, their standard deviations $\sigma_{\Delta\delta}$, $\sigma_{\Delta\theta_1}$, and $\sigma_{\Delta h_1}$ are the quantities of most interest. If we assume that the errors in θ_1, δ, and h_1 are mutually independent we have

$$\sigma_{\Delta r}^2 = \left(\frac{\partial r}{\partial \theta_1}\right)^2 \sigma_{\Delta\theta_1}^2 + \left(\frac{\partial r}{\partial h_1}\right)^2 \sigma_{\Delta h_1}^2 + \left(\frac{\partial r}{\partial \delta}\right)^2 \sigma_{\Delta\delta}^2 \qquad (2.2.2)$$

If the remainder after the first order terms in the Taylor expansion is not negligible, Δr cannot be linearly related to the errors in the input variables and the situation is obviously much more complex. In general it is necessary to examine the remainder and determine for what ranges of the variables it is negligible. In most instances in the subsequent error analyses it will prove adequate to consider only ranges of the variables where the linear relationship is valid.

The remainder in the expansion (2.2.1) can be written as

$$\frac{1}{2}\left[\left(\frac{\partial^2 r}{\partial \theta_1^2}\right)(\Delta\theta_1)^2 + \left(\frac{\partial^2 r}{\partial h_1^2}\right)(\Delta h_1)^2 + \left(\frac{\partial^2 r}{\partial \delta^2}\right)(\Delta\delta)^2 + 2\frac{\partial^2 r}{\partial \theta_1 \partial \delta}\Delta\theta_1\Delta\delta + 2\frac{\partial^2 r}{\partial \theta_1 \partial h_1}\Delta\theta_1\Delta h_1 + 2\frac{\partial^2 r}{\partial \delta\, \partial h}\Delta\delta\Delta h_1\right]_{\tilde{\theta}_1, \tilde{h}_1, \tilde{\delta}}.$$

In this expression the derivatives are to be evaluated at some point $\tilde{\theta}_1$, $\tilde{h}_1$, $\tilde{\delta}$ satisfying

$$\theta_1 \leq \tilde{\theta}_1 \leq \theta_1 + \Delta\theta_1$$
$$h_1 \leq \tilde{h}_1 \leq h_1 + \Delta h_1$$
$$\delta \leq \tilde{\delta} \leq \delta + \Delta\delta$$

but not otherwise determinable.

It is well to note that the sensitivity of the range to a given parameter as exemplified by the partial derivatives is a function not only of the geometrical configuration as shown in Figure 2.1-2 but of the choice of variables to be measured for the determination of r.

A simple example which very clearly illustrates the importance of this point in an error analysis, and which also illustrates the determination of a region of validity for a linear error relation, is the following. Suppose we are given the right triangle shown in Figure 2.2-1 and are asked to determine the length a by measuring b and θ or b and c. Let us assume our only errors occur in measuring b. In the first case we must use the equation

$$a = b \tan \theta$$

and the error

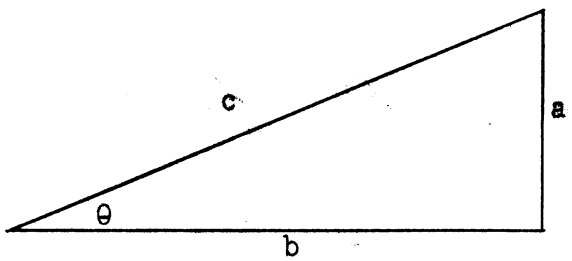

Figure 2.2-1

analysis yields

$$\Delta a = \Delta b \tan \theta .$$

The remainder is zero. In the second case

$$a = \sqrt{c^2 - b^2}$$

and

$$\Delta a \sim - \Delta b \cot \theta \left\{ 1 + \frac{\Delta b}{2\tilde{b}} \frac{c^2}{c^2 - \tilde{b}^2} \right\}, \quad b < \tilde{b} < b + \Delta b .$$

We shall assume that any measurement in which $\tilde{b}^2$ exceeds c^2 is automatically rejected. Then the condition that the magnitude of the remainder be negligible leads to

$$\sin^2 \theta \gg \frac{\Delta b}{b} .$$

Subject to this inequality we have

$$\Delta a = - \Delta b \cot \theta .$$

The formulas show formally that the effect of errors in the measurement of b and either θ or c are serious for small θ in the second case but not in the first case; conversely for large θ. That this should be expected is evident from the fact that for small θ, tan θ is a slowly varying function of θ but c and b are nearly equal so that in the second case one is taking the difference of two nearly equal numbers. On the other hand for θ near 90°, tan θ is very rapidly varying but b and c are quite unequal. Hence, from Equation (2.1.5)

$$\Delta r \sim \frac{r^2\cos\theta_1}{h_1}\,\Delta\theta_1\left[1+\Delta\theta_1\left(\frac{\tilde r}{\tilde h_1}\cos\tilde\theta_1-\frac{1}{2}\tan\tilde\theta_1\right)-\frac{\Delta\delta}{2}\,\frac{\tilde r}{\tilde h_1^{\,2}}\,\frac{\Delta h_1}{\tilde h_1}\,(2\tilde H+1)\right]$$

$$+\frac{2r\bar h}{h_1^{\,2}}\,\Delta h_1\left[1+\frac{\Delta h_1}{2}\,\frac{\tilde H^2}{\tilde h}-\Delta\delta\,\frac{\tilde r}{\tilde h_1^{\,2}}\right]-\frac{r^2}{2h_1^{\,2}}\,\Delta\delta\left[1-\Delta\delta\,\frac{\tilde r}{4\tilde h_1^{\,2}}-2\,\frac{\Delta h_1}{\tilde h_1}\right]. \qquad (2.2.3)$$

In these equations $\bar h = \dfrac{2h_1 + r\sin\theta_1}{2}$, $H = \dfrac{h_1 + r\sin\theta_1}{h_1}$, $\tilde{\bar h} = \dfrac{2\tilde h_1 + \tilde r\sin\tilde\theta_1}{2}$, $\tilde H = \dfrac{\tilde h_1 + \tilde r\sin\tilde\theta_1}{\tilde h_1}$, and $\tilde r = r(\tilde\theta_1, \tilde h_1, \tilde\delta)$. In order to achieve this relatively simple form we have assumed that $\dfrac{r^2}{h_1}\cos\theta_1$, $\dfrac{2r\bar h}{h_1^{\,2}}$ and $\dfrac{r^2}{2h_1^{\,2}}$ were approximately constant in the region from θ_1, h_1, δ to $\theta_1+\Delta\theta_1$, $h_1+\Delta h_1$, and $\delta+\Delta\delta$. This requires that in these intervals h_1 is bounded away from 0 and θ_1 from 90°. In addition it was assumed that $\delta^2 \ll 4h_1^{\,2}$.

Conditions under which the expansion is simply linear in $\Delta\theta_1$, Δh_1, and $\Delta\delta$ are

$$\text{(a)}\quad \left|\frac{2\,\Delta h_1}{\tilde h_1}\right| \ll 1 \rightarrow \left|\frac{\Delta h_1}{h_1}\right| \ll \frac{1}{2}$$

$$\text{(b)}\quad \frac{\tilde r}{\tilde h_1^{\,2}}\,\Delta\delta \ll 1 \rightarrow \frac{r+|\Delta r|}{\tilde h_1^{\,2}}\,\Delta\delta \ll 1 \qquad (2.2.4)$$

$$\text{(c)}\quad \frac{\Delta h_1}{\tilde h_1}\,(2\tilde H+1) \ll 1 \qquad \text{(d)}\quad \frac{\Delta h_1}{\tilde{\bar h}}\,\frac{\tilde H^2}{2} \ll 1$$

$$\text{(e)}\quad \Delta\theta_1\left|\frac{\tilde r}{\tilde h_1}\cos\tilde\theta_1-\frac{1}{2}\tan\theta_1\right| \equiv \Delta\theta_1\left|y(\theta_1;\ \tilde r/\tilde h_1)\right| \ll 1.$$

With any reasonable height measurements condition (a) is always satisfied. From the basic geometry we can certainly expect that $|\Delta r| < r$ so that b may be replaced by

$$(b') \quad \Delta\delta \ll \frac{h_1^2}{2r}$$

which requires that δ be more accurately measured as range increases for the first order approximation to hold. For $\theta_1 = 0$, however, it is not a very restrictive bound, becoming

$$\frac{\Delta\delta}{\delta} \ll \frac{1}{4} .$$

Next consider (e). The function $Y(\theta_1) \equiv y(\theta_1; \tilde{r}/\tilde{h_1})$,

$$Y = \frac{r}{h_1} \cos\theta_1 - \frac{1}{2}\tan\theta_1 \text{ (see Fig. 2.2-3),}$$

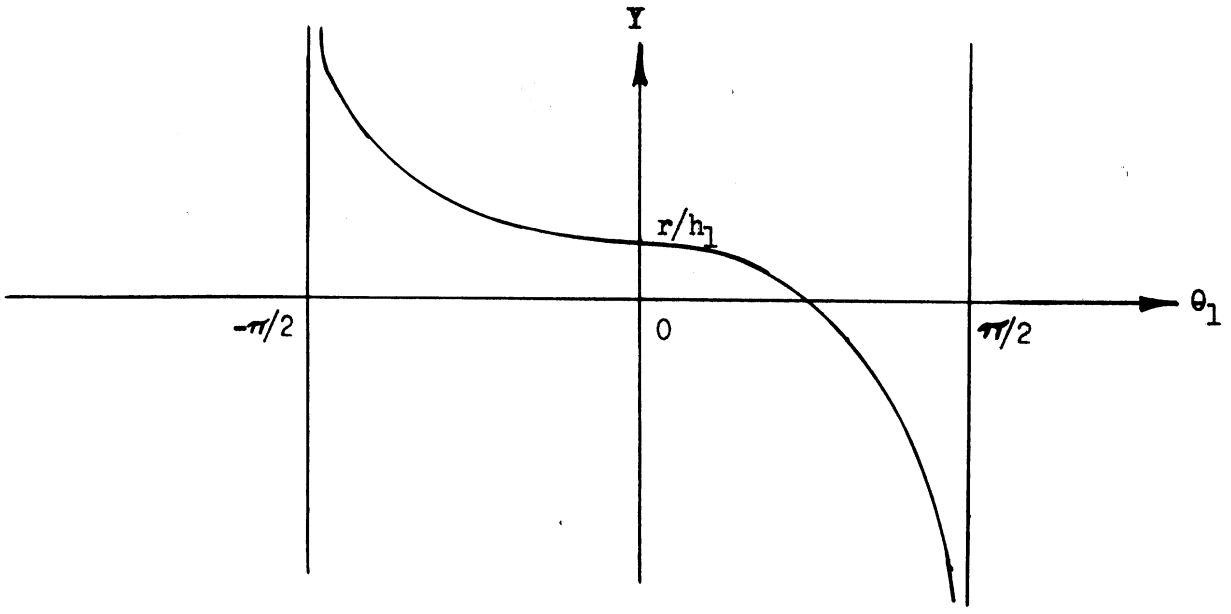

Figure 2.2-3

is monotone decreasing as shown. For $\theta_1 > 0$ it crosses the Y = 0 axis at

$$\theta_1 \sim \arcsin\left(1 - \frac{h_1}{4r}\right) \equiv \theta_o \ .$$

Also we have

$$Y(-\theta_o) = \frac{2r}{h_1}\cos\theta_o = \sqrt{\frac{2r}{h_1}\left(1 - \frac{h_1}{8r}\right)} \ .$$

If

$$|\theta_1| < \theta_o = \arcsin\left(1 - \frac{h_1}{4r}\right)$$

and

$$1 \gg \Delta\theta_1 \sqrt{\frac{2r}{h_1}\left(1 - \frac{h_1}{8r}\right)}$$

condition (e) is satisfied. Now $\frac{h_1}{r} < 1$ so that $\theta_o > 48^\circ$ always; generally it is much larger. Furthermore, let us say $\frac{r}{h_1} > 30^\circ$, then the second inequality yields

$$\Delta\theta_1 \ll .04 \text{ rad},$$

another restriction which should always be satisfied in any practical situation, but which may be lightened for smaller $\frac{r}{h_1}$.

2.3 Effect of the Curvature of the Earth

Before making use of the expression obtained for the error in the preceding section we discuss the effect of neglecting the curvature of the earth.

Referring to Figure 2.3-1 we see that one effect of neglecting the angle ψ (i.e., assuming ψ is zero) is the same as making an error in determining θ_1.

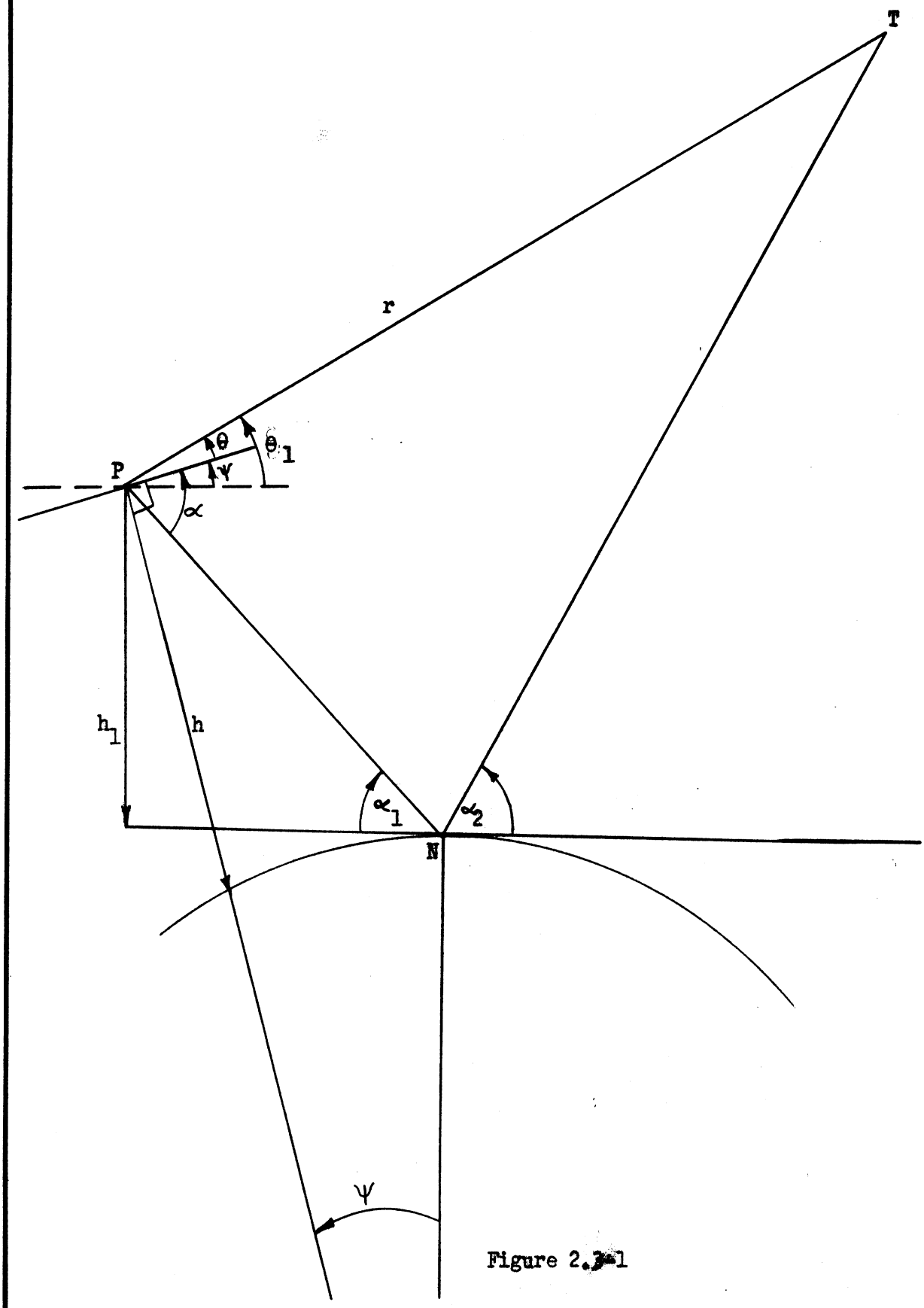

Figure 2.3-1

If ψ is not taken into account the resulting computed range is always too short by an amount

$$\Delta r \sim \frac{r^2}{h}\psi \sim \frac{r^2}{h}\,\frac{r}{2R} = \frac{r^3}{2Rh} \qquad (2.3.1)$$

for small θ_1. R = radius of the earth.

Equations which take the curvature of the earth into account exactly are derived with reference to Figure 2.3-1 as follows:

The quantities which are measurable in the PADAR aircraft are really θ and h rather than θ_1 and h_1. The quantities θ_1, h_1, and α_1 are related to θ, h, and α by

$$\theta_1 = \psi + \theta, \qquad (2.3.2)$$

$$h_1 = (R + h)\cos\psi - R, \qquad (2.3.3)$$

and

$$\alpha_1 = \alpha - \psi. \qquad (2.3.4)$$

In addition to these equations we have

$$(R + h_1)\tan\psi \tan(\alpha - \psi) = h_1. \qquad (2.3.5)$$

Equations (2.1.2), (2.1.3), (2.3.2), (2.3.3), (2.3.4) and (2.3.5) are six independent equations involving the six unknowns, r, θ_1, α_1, h_1, α and ψ ; the parameters to be measured, δ, θ, and h; and the known quantity R. Hence, in principle, they can be solved simultaneously and an equation obtained for r in terms of δ, θ, h and R. However, θ_1 and α_1 may be eliminated immediately leaving only four equations in the unknowns, r, h_1, α and ψ.

2.4 Magnitude of Errors

2.4.1 Bias Errors Due to Earth's Curvature

An approximate determination of the effect of neglecting the earth's curvature is given in the following table, computed using Equation (2.3.1) and r and h combinations satisfying Equation (2.1.5) with $\Delta t = 2.5\mu$sec.

h miles	r miles	r/h	$\frac{\Delta r}{r}$
1.9	15.4	8.1	.02
3.8	61.6	16.2	.1
5.7	139	24.4	.4
7.6	222	29.2	.8

Table 2.4-1

2.4.2 Random Errors

To get orders of magnitude to be expected for $\frac{\sigma_{\Delta r}}{r}$ let us assume $\theta \sim 0$. We shall assume that the altimeter reading for h will lead to $\frac{\sigma_{\Delta h}}{h} \sim .01$*. Let us assume that Δt is being read near the smallest readable value so that we might expect $\frac{\sigma_{\Delta \delta}}{\delta} \sim .1$. The accuracy of reading δ will depend greatly on the steepness of the leading edge of the transmitted pulse and on the terrain roughness. There will be a minimum error

*This error will be larger over hilly terrain or cities with tall buildings.

of approximately $\frac{1}{4}^{o}$ = .004 rad in a stable table determination of the horizontal. The accuracy of determining θ, once a reference horizontal is fixed, is at best about $\sigma_{\Delta\theta}$ = .001 rad so that $\sigma_{\Delta\theta}$ = .005 is an estimate of the accuracy in the θ measurement. We obtain the net result of these errors from the equations of (2.2)

$$\frac{\sigma_{\Delta r}}{r} = \left(\frac{r^2}{h^2} 25 \times 10^{-6} + 4 \times 10^{-4} + .01 \right)^{1/2} .$$

This yields the results given in Table 2.4-2.

r/h	$\frac{\sigma_{\Delta r}}{r}$
2	.1
10	.1
25	.2
50	.3

Table 2.4-2

The portion of these errors which is not due to error in the stable table determination of the horizontal can be further reduced by smoothing. However, at the longer ranges this unreducible angular error is the dominant source of the error. These errors give an idea of the accuracy which might be expected over fairly level horizontal terrain or moderately calm seas.

It should be pointed out that the derivatives such as $\frac{\partial r}{\partial h}$ can be obtained from the equations for a curved earth by differentiating each of the final set of equations arrived at in Section 2.3 with respect to the independent variable in question, h, then solving the resulting set of four linear equations in $\frac{\partial \psi}{\partial h}$, $\frac{\partial h_1}{\partial h}$, $\frac{\partial \alpha_1}{\partial h}$, $\frac{\partial r}{\partial h}$ and $\frac{\partial r}{\partial h}$. In this way a more accurate but far more complicated expression than Equation (2.2.3) for the effects of errors can be obtained.

2.5 Terrain Considerations

Over rolling, or flat but sloping, terrain the above numerical error analysis is not applicable. It is based on the ground level lying perpendicular to the radius of the earth. Any deviation from this plane is essentially a non-measurable error in θ in addition to the ones considered previously.

It is therefore evident that quite small slopes of only 1° or 2° can easily shoot the relative error in range above 100 per cent. If the ground is simply rough or rolling up and down on a short enough scale the error will very likely be essentially random but often with a non-zero mean which puts a bias on the results even when the fluctuations are smoothed out. Long paths along a smooth slope in one direction will similarly give a bias error.

If PADAR is to be used with good results over sloping terrain (which would be quite common over land) it is necessary to measure the

angle α. The new geometric situation is shown in Figure 2.5-1*. A straightforward generalization of the previous set of equations leads to the replacement of Equations (2.1.2) and (2.1.3) by

$$\delta = \frac{h_1}{\sin\alpha_1} + \frac{h_1 + r\sin\theta_1}{\sin\alpha_2} - r \qquad (2.5.1)$$

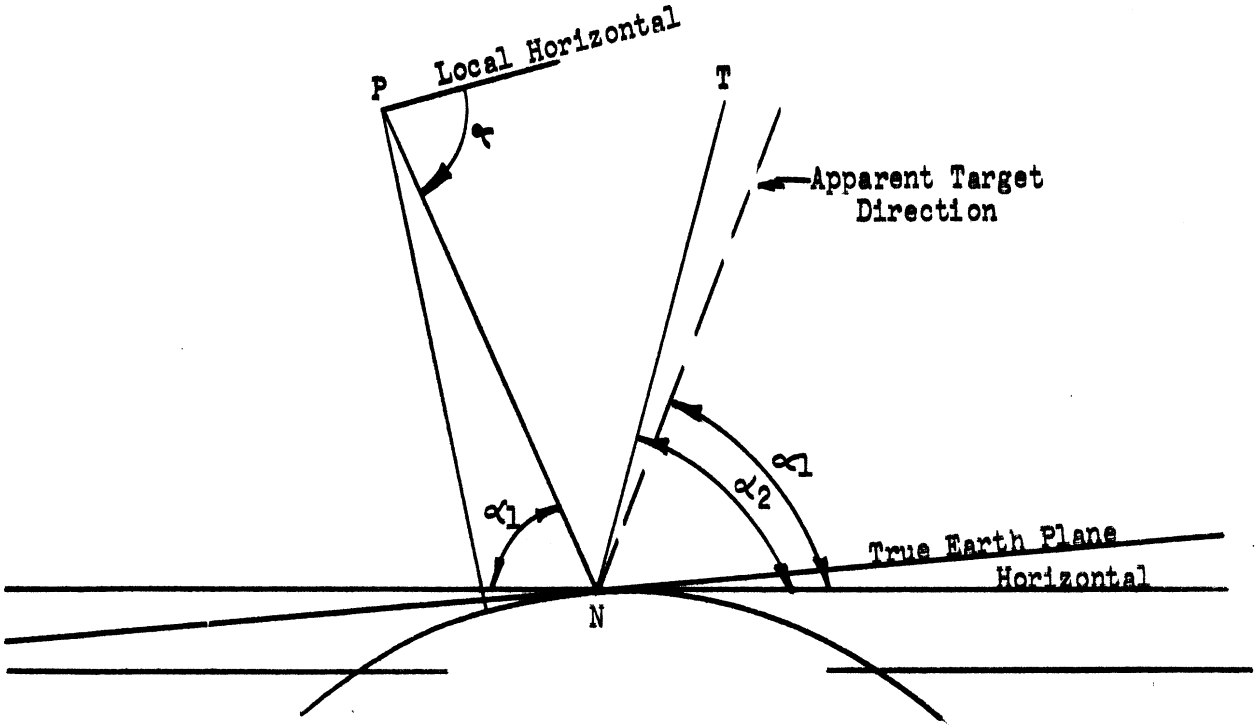

Figure 2.5-1

*In what follows the normal to the sloping surface has been chosen to be in the plane defined by P, N, and T. If the slope has a component perpendicular to this direction, the equations involving α are no longer valid. However, the effect of such a component on range error is much less than that of a comparable component in the plane (for small slopes) and thus the equations derived will still be approximately correct.

$$r \cos \theta_1 = \frac{h_1}{\tan \alpha_1} + \frac{h_1 + r \sin \theta_1}{\tan \alpha_2} \qquad (2.5.2)$$

Equations (2.3.2) through (2.3.5) still hold. These equations now involve the unknowns r, θ_1, α_1, α_2, h_1, and ψ in terms of R and the parameters δ, θ, h, and α to be measured.

In general an accurate measurement of α will be difficult and it is not easy to give an estimate of the effect of this error.

The following relatively simple set of equations may be used instead of the above to determine range when α is measured. In this case, the significant parameters are $\phi = \theta + \alpha$ and $\omega = \frac{\pi}{2} - \alpha$. From Figure 2.5-2 we have

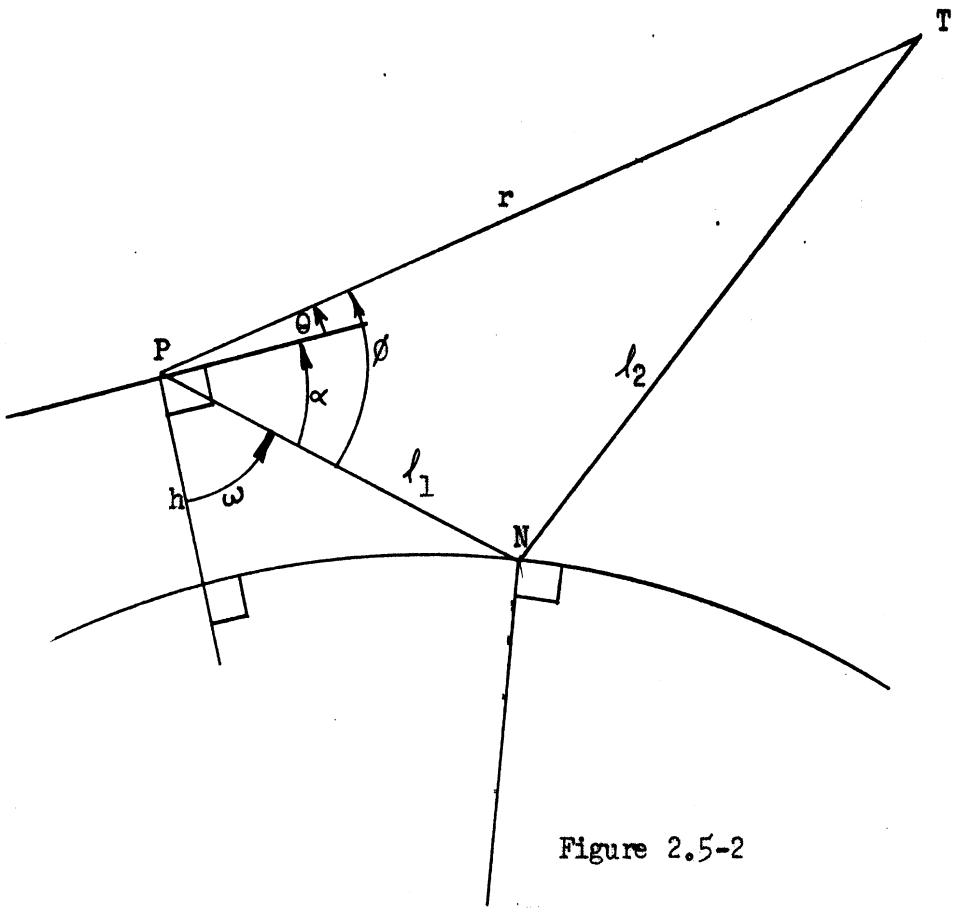

Figure 2.5-2

$$(R + h)^2 + \ell_1^2 - 2\ell_1 (R + h) \cos \omega - R^2 = 0, \tag{2.5.3}$$

$$\ell_1^2 + r^2 - 2r\ell_1 \cos \phi - \ell_2^2 = 0 . \tag{2.5.4}$$

Combining these with

$$\ell_1 + \ell_2 - r - \delta = 0 \tag{2.5.5}$$

yields three independent equations for the unknowns ℓ_1, ℓ_2, and r in terms of the measurable quantities ϕ, ω, h, and δ and the parameter R. By implicit differentiation of these equations we find

$$\frac{\partial r}{\partial \phi} = \frac{r\ell_1 \sin \phi}{\ell_2 - r + \ell_1 \cos \phi} \tag{2.5.6}$$

$$\frac{\partial r}{\partial \omega} = - \frac{(R + h)\ell_1 \sin\omega (\ell_2 + \ell_1 - r \cos \phi)}{[\ell_1 - (R+h) \cos\omega](\ell_2 - r + \ell_1 \cos \phi)} \tag{2.5.7}$$

$$\frac{\partial r}{\partial h} = \frac{[-(R+h) + \ell_1 \cos\omega] (\ell_2 + \ell_1 - r \cos \phi)}{[\ell_1 - (R+h) \cos\omega](\ell_2 - r + \ell_1 \cos \phi)} \tag{2.5.8}$$

$$\frac{\partial r}{\partial \delta} = \frac{-\ell_2}{\ell_2 - r + \ell_1 \cos \phi} \tag{2.5.9}$$

$$\frac{\partial r}{\partial R} = \frac{-(h - \ell_1 \cos \omega)(\ell_2 + \ell_1 - r \cos \phi)}{[\ell_1 - (R+h) \cos\omega] (\ell_2 - r + \ell_1 \cos \phi)} \tag{2.5.10}$$

We shall compare the orders of magnitude of these derivatives with those obtained for a flat horizontal earth when $\theta \sim 0$ (see Eq. 2.2.3). We let ϕ be small, and $\omega \sim \frac{\pi}{2} - \phi$. Then $\phi \sim 2h/r$. Also we shall assume $\ell_2 \sim \ell_1 \sim r/2$ (i.e., $\alpha_1 = \alpha_2$). Then we have

$$\frac{\partial r}{\partial \phi} \sim -\frac{r^2}{h}; \quad \frac{\partial r}{\partial \omega} \sim \frac{2R\, r^2}{r^2 - 4Rh}$$

$$\frac{\partial r}{\partial h} \sim \frac{4Rr}{r^2-4Rh}; \quad \frac{\partial r}{\partial \delta} \sim \frac{r}{2\delta} \sim \frac{r^2}{2h^2}; \quad \frac{\partial r}{\partial R} \sim \frac{16h^3}{3r(r^2-4Rh)}$$

$$\frac{\Delta r}{r} = \frac{1}{r}\frac{\partial r}{\partial \delta}\Delta\delta = \frac{1}{2}\,\frac{\Delta\delta}{\delta}\ .$$

In the limit as $R \longrightarrow \infty$, for $\theta = 0$ and $\alpha_1 = \alpha = \phi$, these coefficients are of the same order of magnitude as, but not equal to, those given in Equation (2.2.3) for the same case.

In Equation (2.2.3) we had (for first order terms and $\theta \sim 0$)

$$\frac{\Delta r}{r} = \frac{r}{h}\Delta\theta + \frac{2}{h}\,\Delta h - \frac{1}{\delta}\Delta\delta .$$

In the present case we obtain

$$\frac{\Delta r}{r} = -\frac{r}{2h}\,\Delta\phi - \frac{r}{2h}\,(\Delta\phi + \Delta\omega) - \frac{1}{h}\,\Delta h + \frac{1}{2\delta}\,\Delta\delta .$$

The reason for grouping the angular terms in this fashion is that $\Delta\phi + \Delta\omega = \Delta(\phi + \omega) = \Delta(\frac{\pi}{2} + \theta)$, is precisely $\Delta\theta$. We denote the range as determined by the more complicated technique as $\bar{r}$. Then combining these relative error equations gives

$$\frac{\Delta \bar{r}}{\bar{r}} = -\frac{\bar{r}}{2h}\,\Delta\phi - \frac{1}{2}\,\frac{\Delta r}{r}\,.$$

It will probably not be possible to measure ϕ (which is the direction to a diffuse reflector) with nearly as good accuracy as can be obtained in measuring θ (direction to a transmitter). We regard θ and ϕ errors as uncorrelated and obtain

$$\sigma^2_{\frac{\Delta \bar{r}}{\bar{r}}} = \frac{\bar{r}^2}{4h^2}\,\sigma^2_{\Delta\phi} + \frac{1}{4}\,\sigma^2_{\frac{\Delta r}{r}}\,.$$

This shows that if the assumption concerning the accuracy with which ϕ can be determined is correct, using $\bar{r}$ instead of r will usually lead to increased range errors for the flat earth, equal altitude case.

It is worth mentioning that conventional antenna pointing methods such as conical scan should not be expected to give very good results in determining ϕ since there will generally be no very clearly defined bright spot on the ground standing out from the surroundings and subtending an angle much smaller than is enclosed by the antenna half power points.

The effect of index of refraction variations in the atmosphere in deteriorating the accuracy of α measurements is discussed in the next

section. Here we merely point out another source of error due to refraction; namely, refraction of rays through the radome. This, however, is to a considerable degree under the control of the PADAR equipment designer.

2.6 Effect of Index of Refraction Variations

The index of refraction of the atmosphere is not a constant from point to point. The rays representing the direction of energy propagation are therefore not straight lines but bent.

Because the index of refraction is affected by variations in the temperature and moisture content of the air, it fluctuates considerably near the earth's surface*. In the most extreme case, the phenomenon known as ducting occurs. This is a situation in which rays below about 1° to 2° from the horizontal are to a considerable extent trapped and guided along the earth's surface. There are large regions of the world where this situation is almost always present, others where it occurs at night only, and others where it occurs irregularly. Thus, it appears that PADAR will be unreliable for situations where the angle α must be measured, if the indirect ray is at angles α_1 less than about one degree. Whether or not α is measured, poor results are to be expected from this source for extreme ranges, or for receiver and transmitter at low altitudes (i.e., whenever the direct ray comes close to grazing the earth).

---

* The characteristics of these random effects are undergoing investigation in various quarters.

For greater α_1, the ground layer effects will not predominate. At higher altitudes, fluctuations in the index of refraction tend to be less violent, though ducting is still present at times (and when it occurs may preclude ranging). On the average, the index of refraction falls off fairly continuously with altitude, though large fluctuations are possible. The data appear to be very scarce above a mile or so. The error introduced into the angle measurements by the bending of the rays becomes comparable with the non-refraction angle errors at ranges of the order of eighty miles. Since refraction tends to lengthen all the ray paths, direct and indirect, barring ducting the effect on δ will usually be small.

This discussion is of necessity preliminary. Further analysis and correlation of data and much new experimentation would be required to clear up the propagation picture.

APPENDIX 3

FURTHER APPLICATIONS OF PADAR

3.1 General Considerations

The situations in which the PADAR technique may be used fall naturally into two broad classes. The first involves determination of the range from receiver to transmitter; the second, determination of range from receiver to reflector. The most promising application in the first class appears to be the original PADAR scheme which has been discussed at length in References 1 through 5 and in Appendix 2. The subject of this appendix is applications in which the range of a reflecting object is to be determined. Two such problems will be treated in some detail.

3.2 Applications of PADAR Against Beam-Rider Missile Systems

3.2.1 Statement of the Beam-Rider Range Problem

The situation to be considered is illustrated in Figure 3.2-1. Consideration of the geometry involved shows that missile range information may be bought only at the price of an increase in the complexity of the system. Determining the range of the attacking missile involves the measurement of the two angles, β and ϕ, analogous to those of Appendix 2 (2.5), rather than the one required in the simple "bounce off the ground" scheme discussed first in Appendix 2. Furthermore, although these are essentially the same measurements made in the modified PADAR technique discussed in Appendix 2 (2.5), the situation is further complicated due to the addition of a new dimension. In the "bounce off the ground"

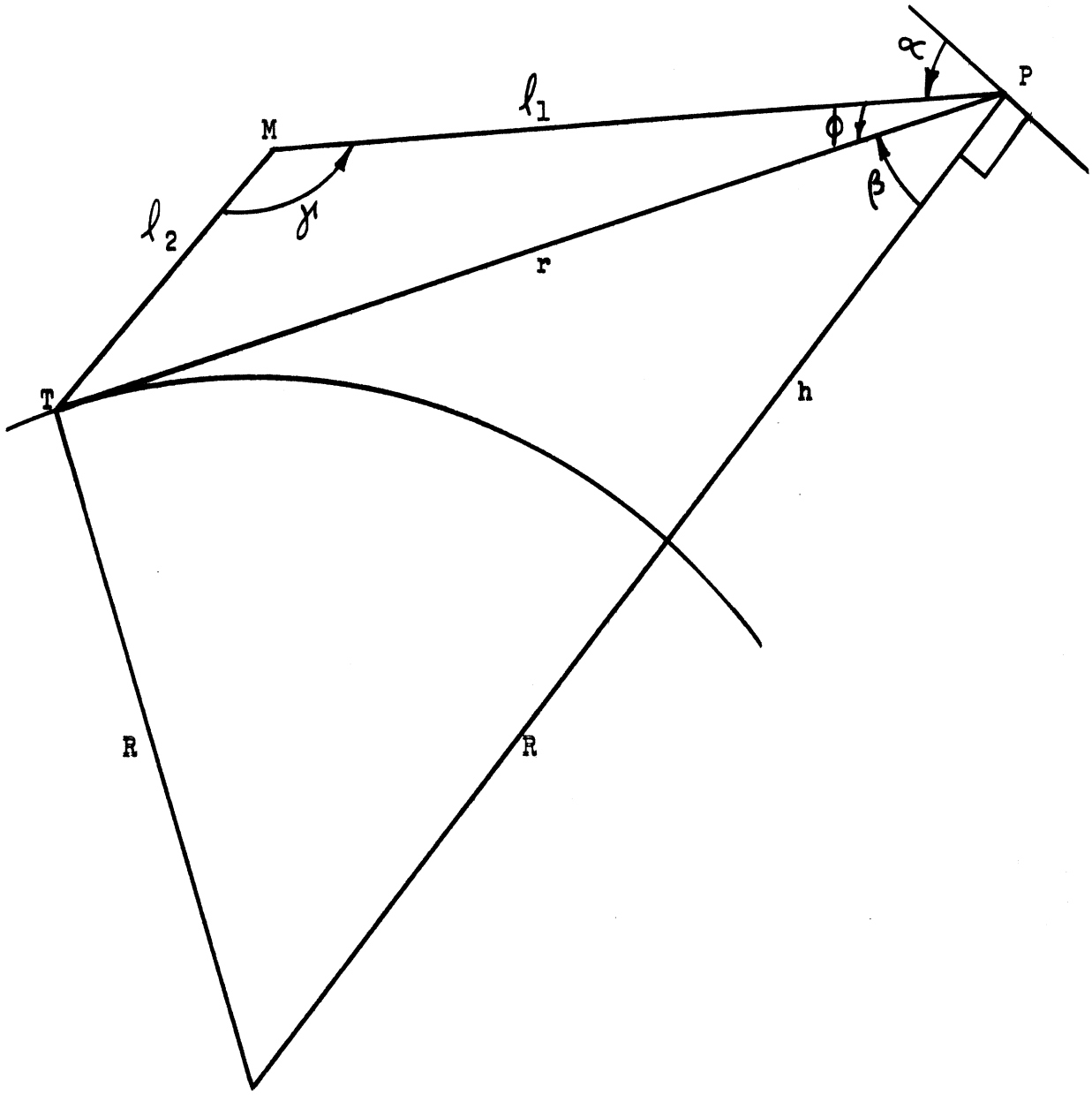

Figure 3.2-1

Note: The plane defined by MPT is the one in which ϕ is measured and it is generally not the vertical plane.

problem, a two-dimensional picture sufficed to approximate the situation since the PADAR airplane, the transmitting airplane and the "bounce point" were assumed to lie in a vertical or nearly vertical plane. Now, the same measurements as before can be made to yield range information. However, an additional measurement is required if the direction of the missile is desired. It should be kept in mind that accurate angular measurement was shown to be the most important requirement for improved PADAR range determination.

Because beam-rider missile systems involve both a tracking radar and a guidance transmitter the question of which of these is providing the PADAR energy must be considered in this application. After the incoming bomber is in the direct beam of the tracking radar, the missile is launched in the beam of a guidance transmitter and the guidance beam is brought into conjunction with the tracking beam. These radars will be assumed to be operating at different frequencies. Thus, tuning of the PADAR receiver eliminates confusion of the two. Since the beam-width of the tracking radar will generally be very narrow in comparison to the beam-width of the guidance radar, the utilization of the guidance radar in the PADAR technique, despite its lower power, seems to be necessary. Whichever radar is used it is quite possible that because of the absence of sufficiently powerful side lobes, no range determination can be made in time to take any effective action. Information as to the pattern of an enemy transmitter is essential in deciding whether PADAR should be developed for this application. In the absence of this information it will be assumed that

the direct path signal from the transmitter is detectable at the PADAR receiver throughout the interception.

We estimate the minimum missile cross-section such that the incoming bomber can detect the missile at any point along its trajectory. The radar range equation in the form

$$\sigma = \frac{(4\pi)^3 (\ell_1 \ell_2)^2}{\lambda^2 G_1 G_2} \cdot \frac{P_2}{P_1} \qquad (3.2.1)$$

where subscript 1 refers to the transmitter and subscript 2 to the receiver, indicates that for fixed values of the minimum detectable received power P_2, the wavelength, the gains, and the peak transmitted power, an upper bound for the minimum σ will be obtained for the maximum value of $(\ell_1 \ell_2)^2$. We will now specialize to a particular beam-riding missile system, Talos. Choosing the parameters for the missile guidance transmitter on the basis of information given in References 8 and 9 we obtain for the Talos system

$$\sigma \simeq \frac{(4\pi)^3 (\ell_1 \ell_2)^2}{(.0625)\ 10^3\ G_2} \cdot \frac{P_2}{15} \quad \text{ft.}^2 \qquad (3.2.2)$$

$\lambda = .25$ ft ,

$P_2 =$ kw.,

$G_1 = 10^3$

$\ell_1 =$ ft.,

$\ell_2 =$ ft.

Typical maximum values of the product of the ranges, $\ell_1 \ell_2$ should be of

the order of $25 \cdot 10^9$ square feet. The parameters over which the PADAR designer has at least some degree of control are P_2 and G_2. It seems reasonable that a receiver with a gain of about 1000 and a minimum detectable power of 10^{-17} Kw. could be produced. Very roughly then, the order of magnitude of the minimum cross-section to permit ranging the missile throughout its attack is of the order of 1 to 10 square feet. It should be pointed out that this result is far more sensitive to variation of the value of the range product than to that of the other parameters and that if the beam-rider missile has greater range capability than Talos this minimum cross-section increases greatly.

In ordinary PADAR the reflected signal moves away from the direct signal on an A-scope presentation as the range decreases. However, in such applications as this one, the path difference which is being measured tends to zero; hence on an A-scope the reflected signal moves toward the direct signal. This probably increases the difficulties arising from the presence of more than one target. A preliminary calculation indicates that it may be possible to use the Doppler effect to discriminate between different targets.

3.2.2 Error Analysis for the Talos System

With the above general considerations in mind we proceed to determine ranging accuracy for those cases where the angle χ between the transmitter and receiver directions, measured at the missile, is equal to, or greater than 120°. The PADAR carrying aircraft is referred to herein as a bomber.

On the assumption that it is more important to have accurate range information at ranges under 100 miles, only such missile-bomber separations will be considered.

Referring to Figures 2.5-2 and 3.2-1 we observe that the algebraic manipulation involved in obtaining the unknown distance is the same in both cases. Substituting β for ω and interchanging r and ℓ_1 in Equation (2.5.3) gives us, with the help of Equations (2.5.4) and (2.5.5) which still apply, a system of equations from which ℓ_1 may be determined.

$$\ell_1 + \ell_2 - r = \delta \tag{3.2.3}$$

$$\ell_2^2 = \ell_1^2 + r^2 - 2\, r\, \ell_1 \cos \phi \tag{3.2.4}$$

$$R^2 = (R + h)^2 + r^2 - 2r(R + h) \cos\beta \tag{3.2.5}$$

from which we obtain

$$\ell_1 = \frac{\delta(\delta + 2r)}{2(\delta + r - r \cos \phi)} \quad . \tag{3.2.6}$$

Writing

$$\ell_1 + \Delta\ell_1 = \frac{(\delta + \Delta\delta)(2r + 2\Delta r + \delta + \Delta\delta)}{2\left[\delta + \Delta\delta + (r + \Delta r)(v + \Delta v)\right]} \tag{3.2.7}$$

where $v = 1 - \cos \phi$, we obtain

$$\Delta \ell_1 = \frac{\delta^2(2-v)\Delta r + [\delta^2 + 2vr(r+\delta)]\Delta\delta - r\delta(2r+\delta)\Delta v}{2(\delta + vr)^2 (1+\varepsilon)}$$

$$+ \frac{2(\delta + vr)\Delta r\Delta\delta + (\delta+vr)\Delta\delta^2 - \delta(2r+\delta)\Delta v\Delta r}{2(\delta + vr)^2(1+\varepsilon)} \qquad (3.2.7)$$

where

$$\varepsilon = \frac{r\Delta v + v\Delta r + \Delta\delta + \Delta v\Delta r}{\delta + rv} .$$

Neglecting second order terms in the errors gives the first order terms of the Taylor series

$$\Delta \ell_1 = \frac{\delta^2(2-v)\Delta r + [\delta^2 + 2vr(r+\delta)]\Delta\delta - r\delta(2r+\delta)\Delta v}{2(\delta + vr)^2} . \qquad (3.2.8)$$

It is necessary to examine the conditions under which this is a good approximation. They are $\frac{\Delta\delta}{r} \ll 1$, $\frac{\Delta\delta}{\delta} \ll 1$, $\frac{\Delta r}{r} \ll 1$ and $\Delta v \ll v + \frac{\delta}{r}$. The last condition corresponds to bounding ϕ away from zero. This is a very natural restriction, since when the missile is along the PADAR-transmitter line of sight no range determination can be made. The bound we will use on ϕ will be: $20\,|\Delta\phi| < \phi$ (which leads to $v > 10\Delta v$). $\Delta\phi$ contains only random errors and should be measurable with good equipment to an accuracy of at least $\pm .1^{\circ}$. This leads to $v > .001$ corresponding to the fourth condition. In virtually all situations of interest, the

Taylor series adequately represents the error in range. Now

$$\Delta v = \sin \phi \Delta \phi \cong \sqrt{v(2-v)}\ \phi.$$

Replacing δ/r by u,

$$\Delta \ell_1 = \frac{1}{2}\left\{ h_1(u,v)\,\Delta r - r\, h_2(u,v)\,\Delta \phi + h_3(u,v)\,\Delta \delta \right\}, \qquad (3.2.9)$$

where

$$h_1(u,v) = \frac{u^2(2-v)}{(u+v)^2}$$

$$h_2(u,v) = \frac{u(u+2)\sqrt{v(2-v)}}{(u+v)^2}$$

$$h_3(u,v) = 1 + \frac{v(2-v)}{(u+v)^2}.$$

In Figures 3.2-2, 3.2-3 and 3.2-4, h_1, h_2, and h_3 are plotted as functions of u and v. These figures may be used to obtain the value of the error in ℓ_1 for any assumed configuration and fixed errors in ϕ, δ, and r, the measured quantities. Furthermore if we regard h_1, h_2, and h_3 as the weights assigned to the errors in measurement, the three figures give an immediate qualitative picture of the importance of each of the error quantities.

As before, the quantities in Equation (3.2.9) are uncorrelated; thus, the standard deviation of the distance $\Delta\ell_1$ is

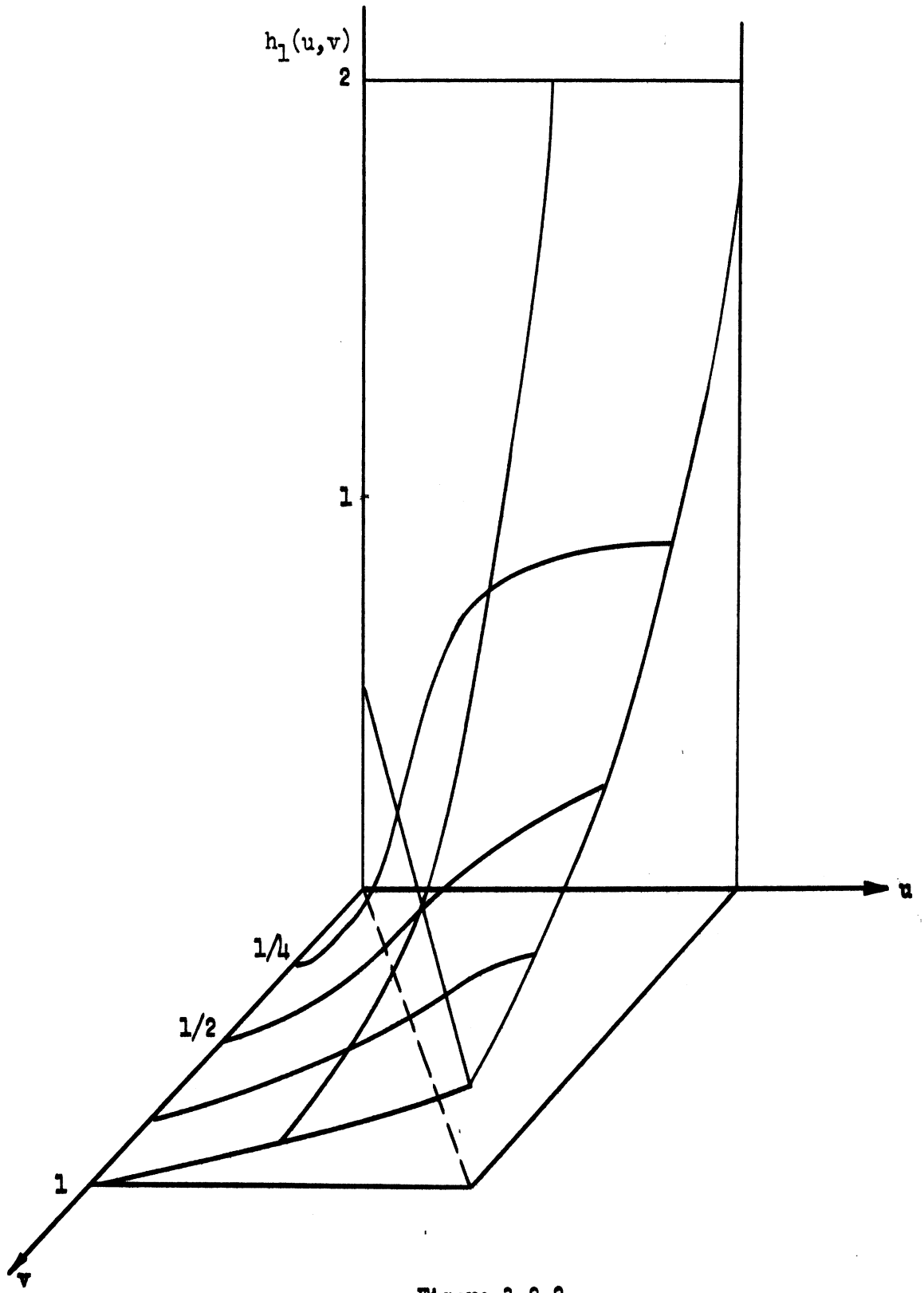

Figure 3.2-2

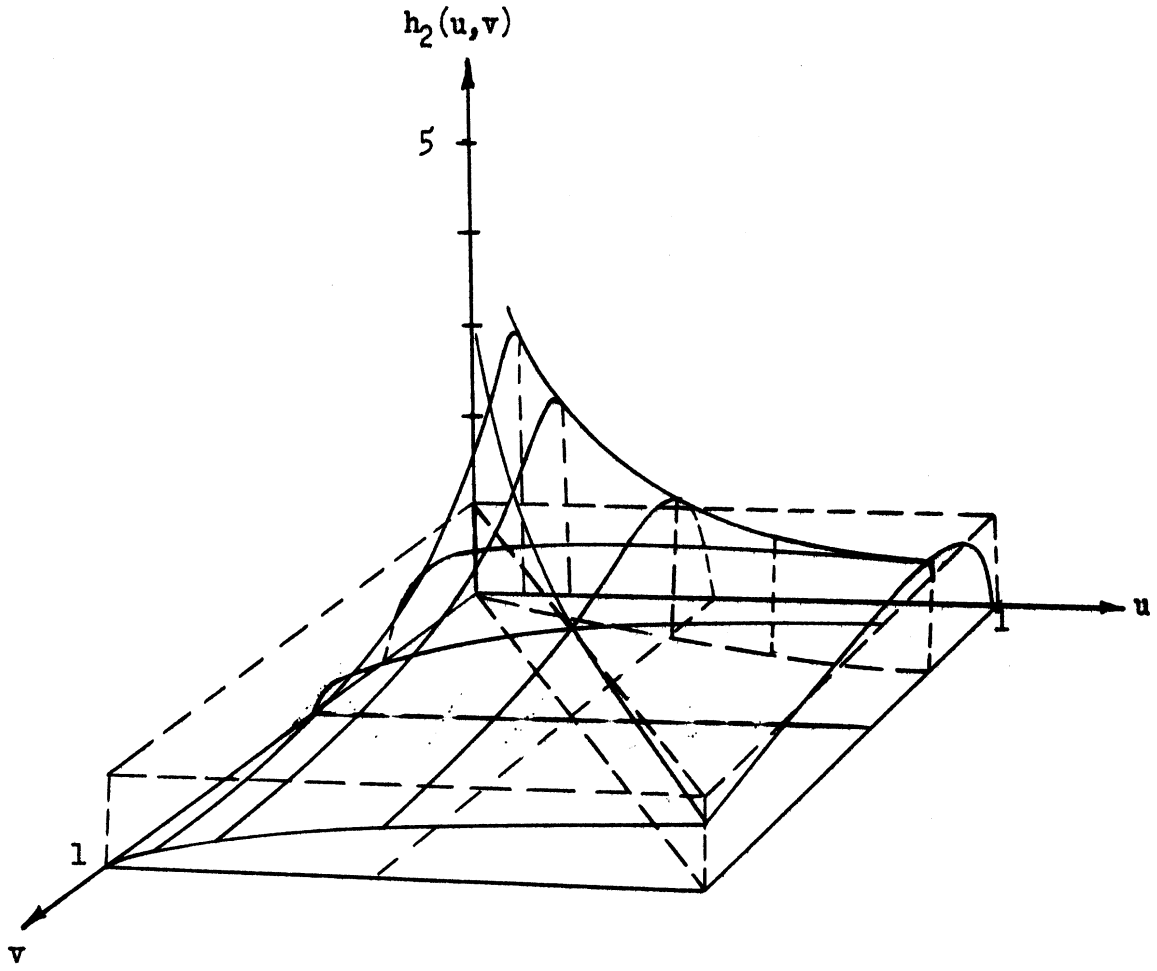

Figure 3.2-3

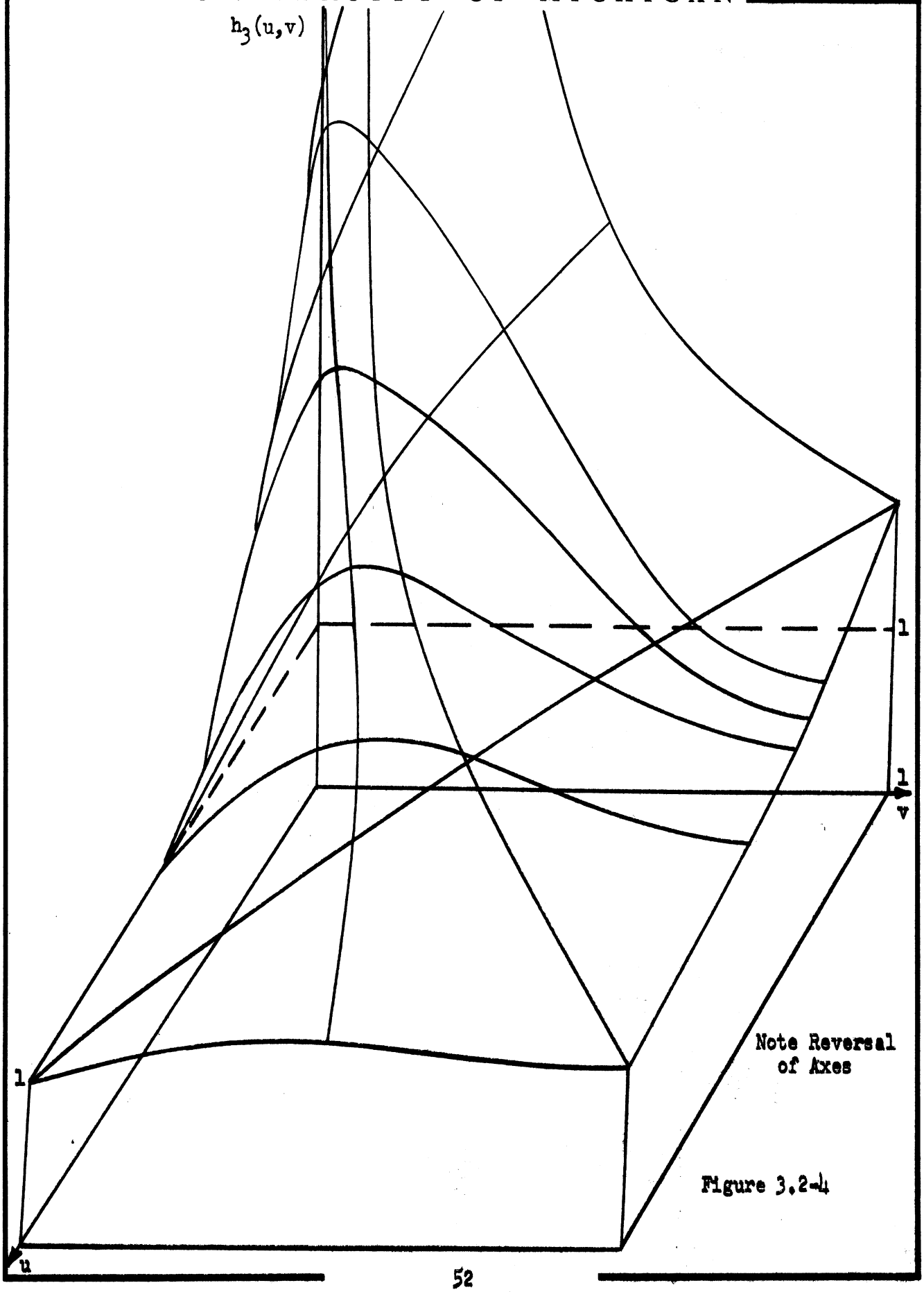

Figure 3.2-4

$$\sigma_{\Delta \ell_1} = \frac{1}{2} \left\{ \left[h_1(u,v)\, \sigma_{\Delta r} \right]^2 + \left[r h_2(u,v)\, \sigma_{\Delta \phi} \right]^2 + \left[h_3(u,v)\, \sigma_{\Delta \delta} \right]^2 \right\}^{1/2} \qquad (3.2.10)$$

To give an explicit example of the sort of errors to be expected a few cases were computed.

Here r was chosen to be 40 miles and ℓ_1 as 15 miles. For the errors, $\sigma_{\Delta r}$ = 1 mile, $\sigma_{\Delta \delta}$ = .01 miles, and $\sigma_{\Delta \phi} = .1^\circ$. This is not a particularly favorable case. The results and the ϕ and δ combinations used are shown in Table 3.2-1.

ϕ	δ	$\sigma_{\Delta \ell_1}$
5°	.091	1.1
10°	.36	.35
15°	.80	.22

Table 3.2-1

In order to compare directly the errors in this case with those occurring when the reflection is from the ground we rewrite $\Delta \ell_1$ in the partial derivative notation

$$\Delta \ell_1 = \frac{\partial \ell_1}{\partial \phi} \Delta \phi + \frac{\partial \ell_1}{\partial \delta} \Delta \delta + \frac{\partial \ell_1}{\partial r} \Delta r \qquad (3.2.11)$$

$$\Delta r = \frac{\partial r}{\partial \beta} \Delta \beta + \frac{\partial r}{\partial h} \Delta h, \qquad (3.2.12)$$

and

$$\frac{\partial r}{\partial \beta} = \frac{r(R + h)\sin\beta}{(R + h)\cos\beta - r} = \frac{\delta + r - r\cos\phi}{\delta - \ell_1 + \ell_1\cos\phi}\,\frac{\partial \ell_1}{\partial \beta} \qquad (3.2.13)$$

$$\frac{\partial r}{\partial h} = \frac{(R + h) - r\cos\beta}{(R + h)\cos\beta - r} = \frac{\delta + r - r\cos\phi}{\delta - \ell_1 + \ell_1\cos\theta}\,\frac{\partial \ell_1}{\partial h} \qquad (3.2.14)$$

Or, analogous to the equation given in Appendix 2 (2.5) for the error

$$\Delta\ell_1 = \frac{\partial \ell_1}{\partial \phi}\Delta\phi + \frac{\partial \ell_1}{\partial \beta}\Delta\beta + \frac{\partial \ell_1}{\partial h}\Delta h + \frac{\partial \ell_1}{\partial \delta}\Delta\delta\,, \qquad (3.2.15)$$

where

$$\frac{\partial \ell_1}{\partial \phi} = -\frac{r\,\ell_1\sin\phi}{\delta + r - r\cos\phi}\,, \qquad (3.2.16)$$

$$\frac{\partial \ell_1}{\partial \beta} = -\frac{(\delta + \ell_1\cos\phi - \ell_1)}{(\delta + r - r\cos\phi)}\,\frac{r(R + h)\sin\beta}{\left[r - (R + h)\cos\beta\right]}\,, \qquad (3.2.17)$$

$$\frac{\partial \ell_1}{\partial h} = \frac{(\delta - \ell_1 + \ell_1\cos\phi)}{(\delta + r - r\cos\phi)}\,\frac{\left[r\cos\beta - (R + h)\right]}{\left[r - (R + h)\cos\beta\right]}\,, \qquad (3.2.18)$$

$$\frac{\partial \ell_1}{\partial \delta} = \frac{\ell_2}{\delta + r - r\cos\phi}\,, \qquad (3.2.19)$$

$$\frac{\partial \ell_1}{\partial r} = \frac{2\ell_1^{\,2}(1 + \cos\phi)}{(\delta + 2r)^2}\,. \qquad (3.2.20)$$

It can be seen that the coefficients in Equation (3.2.15) are generally smaller than the corresponding coefficients in Appendix 2 (2.5)*. In addition, the errors in this case are generally of the same order as those in Appendix 2 (2.5) and in particular the most important error, the one in β, is much smaller because in this case we measure a direction to the transmitter, in the other to a diffuse spot on the ground. Thus it is seen that Equation (3.2.12) yields much smaller range errors than does the corresponding equation of Appendix 2 (2.5) for all cases of interest where Equation (3.2.12) is valid.

If we neglect $\delta/2$ with respect to l_1, then

$$\frac{\partial l_1}{\partial \phi} \sim -\frac{l_1^2 \sin \phi}{\delta} \tag{3.2.21}$$

$$\frac{\partial l_1}{\partial \delta} \sim \frac{l_1 l_2}{r \delta} \tag{3.2.22}$$

$$\frac{\partial l_1}{\partial \beta} \sim \frac{l_1^2}{r^2} \frac{\partial r}{\partial \beta} \tag{3.2.23}$$

$$\frac{\partial l_1}{\partial h} \sim \frac{l_1^2}{r^2} \frac{\partial r}{\partial h} \tag{3.2.24}$$

$$\frac{\partial l_1}{\partial r} \sim \frac{l_1^2 (1 + \cos \phi)}{2r^2} \tag{3.2.25}$$

*We omit $\frac{\partial l_1}{\partial R} R$ which is always small in this case.

These approximations are very useful in the case in which the beam-rider missile follows a trajectory near the transmitter-PADAR line of sight. In the case of an up and over trajectory $\delta/2$ is not always negligible with respect to l_1.

3.3 Application of PADAR to a Reflecting Target Experiment

3.3.1 Description of the Experiment

It has been proposed by the United States Air Force that some experimental evidence clarifying the feasibility of obtaining range information on a reflecting target could be obtained with the use of readily available equipment. Referring to Figure 3.3-1, in the proposed experiment one F-86D aircraft irradiates another, and the present Fairchild PADAR equipment (modified so as to be able to obtain the appropriate angular measurements) makes range measurements.

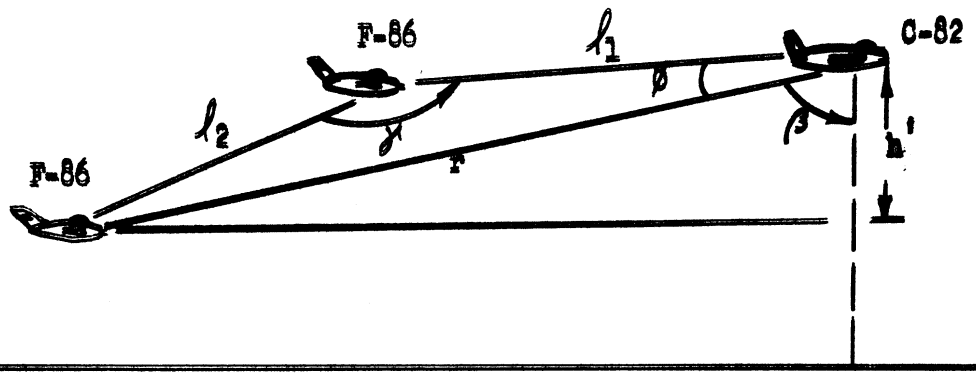

Figure 3.3-1

In principle, range information can be obtained in this situation; the problem differs from the one discussed in Appendix 3 (3.2) in that one less piece of information is available -- the height of the transmitter (or equivalent information) must be supplied to the PADAR carrying airplane. The governing equations are very similar to those determined in Appendix 3 (3.2.2); they are

$$\ell_1 = \frac{\delta(2r + \delta)}{2[\delta + r(1 - \cos\phi)]} \qquad (3.3.1)$$

$$r \equiv \frac{h'}{\cos\beta} \quad . \qquad (3.3.2)$$

3.3.2 Detectability of Reflection

The reflected power received can be determined from the following form of the radar range equation

$$P_2 = \frac{\lambda^2 P_1 G_1 G_2 \sigma}{(4\pi)^3 (\ell_1 \ell_2)^2} \qquad (3.3.3)$$

where:

P_1 = transmitted power (200 kw)

G_1 = transmitter gain (10^3, assumed)

G_2 = receiver gain (900)

λ = wavelength (3 cm)

σ = cross-section of the reflector

Values of these parameters for the E-4 fire control system of the F-86D and the APS-4 receiver utilized in the Fairchild PADAR aircraft were obtained from Reference 10. The range r is assumed to be fifty miles or less. Reference to Appendix 1 shows that for the angle γ restricted to a range greater than 120°, the minimum radar cross-section of the F-86D is about $3ft^2$.

The largest value of $\ell_1 \ell_2$ is approximately $625\ mi^2$. From Equation (3.3.3) we get

$$P_2 \gtrsim 10^{-17} kw.$$

Comparing with the minimum detectable signal of 10^{-16}kw for the APS-4 receiver, we see that for detection of the reflected signal at least a factor of 10 must be picked up. That is, the quantity $\sigma / \ell_1^2 \ell_2^2$ must be at least $10 \left[\sigma_{min}/(\ell_1 \ell_2)^2_{max}\right]$. Hence at ranges $\ell_1 \cong \ell_2 \cong 25$ mi, σ must be at least $30\ ft^2$. Referring to the cross-section data of Appendix 1 one sees that for the cone $\zeta = 20^{\circ}$, the smallest cross-section is $98ft^2$; on the cone $\zeta = 30^{\circ}$ the cross-section is above $30ft^2$ for ξ between 0° and 20° and between about 55° and 180°; for $\zeta = 40^{\circ}$, 50°, and 60°, $\sigma > 30ft^2$ only for a very limited range of the angle ξ.

Hence on the basis of these numbers, we would expect the reflected signal to be detected when $\ell_1 = \ell_2 = 25$ mi, over all aspects of the cone $\zeta = 20^{\circ}$, over about 3/4 of the cone $\zeta = 30^{\circ}$, and essentially not detectable on the larger cones. We point out that usually radar sets do

not operate at 100% efficiency, the degradation tending to reduce the expected ratio of received signal to noise. Also the cross-section values are only calculated to an accuracy of $\pm$ 10db (a factor of 10).

Taking into account these uncertainties, we make the following rough predictions concerning the detection of the reflected echo. Let us define the instrument degradation factor, $\mathcal{K}/\mathcal{K}'$ where $\mathcal{K} = \frac{P_1 G_1 G_2}{P_N}$, where P_N = noise power in the receiver as given in the instrument specifications, P_t, G_t, and G_r are the values also given in the specifications; $\mathcal{K}' = \frac{P_1' G_1' G_2'}{P_N'}$, the primes indicating actual values obtained in practice. We will not consider high, narrow peaks in the computed cross-section as being significant, since comparisons (Ref. 6) of previous theoretical computations with experiment show that these peaks are generally too high.

On the basis of the assumption that $\frac{\mathcal{K}}{\mathcal{K}'} \leq 2$, we will predict sure signal detection if the computed received power, P_2, divided by $10\,\mathcal{K}'$ is greater than P_N; fair probability of detection if $\frac{P_2}{10\mathcal{K}'} < P_N < \frac{P_2}{\mathcal{K}'}$; no prediction when $\frac{P_2}{\mathcal{K}'} < P_N < \frac{10P_2}{\mathcal{K}'}$; low probability of detection if $\frac{10P_2}{\mathcal{K}'} < P_N$.

$\underline{\ell_1 \cong \ell_2 \cong 25 \text{ miles};\ \mathcal{K}/\mathcal{K}' \leq 2}$

Since $\mathcal{K}/\mathcal{K}'$ is assumed ≤ 2, $\sigma \geq 60\text{ft}^2$ will be detected.

$\underline{\gamma = 20^\circ}$

If all the computed cross-sections were a factor of ten too large, there would be no detection. If $\sigma \cong \frac{1}{5}\,\sigma_c$ (σ_c is the computed cross-section) the echo would be detected at about half the aspects on this 20° cone.

Conclusion: Fair probability of detection at most aspects.

$\gamma = 30^\circ, 40^\circ, 50^\circ, 60^\circ$

No prediction.

$l_1 \cong l_2 \cong 15$ miles; $\kappa/\kappa' \leq 2$

Detection if $\sigma_c \geq 80 ft^2$.

$\gamma = 20^\circ$

Detection at all aspects.

$\gamma = 30^\circ$

Detection at ξ : ~ 10°, 60° to 100°, 170° to 180°.

$\gamma = 40^\circ, 50^\circ$

Fair probability of detection at most aspects.

$\gamma = 60^\circ$

No prediction.

$l_1 \cong l_2 \cong 10$ miles; $\kappa/\kappa' \leq 2$

Detection if $\sigma_c \geq 15 ft^2$.

$\gamma = 20^\circ$

Detection at all aspects.

$\gamma = 30^\circ$

Detection at all aspects.

$\gamma = 40^\circ$

Detection at ξ : 0° to 25°; 70° to 85°; 140° to 180°

$\gamma = 50^\circ$

Detection at ξ: 10° to 20°; 160° to 180°. Fair probability of detection at most aspects.

$\delta = 60^{\circ}$

Fair probability of detection at most aspects.

$\ell_1 \cong \ell_2 \cong 5$ miles

Detection if $\sigma_0 \geq 1$ square foot . Detection at all aspects even if κ/κ' is as great as 6.

3.3.3 Errors in Range for the Experiment

The equations governing range determination in the proposed experiment differ from those derived for the problem of determining the range of a beam-rider missile in only one particular. In the experiment it would be necessary to provide the PADAR with information to make up for the fact that its altitude relative to the transmitter can no longer be computed since it is proposed that an airborne transmitter be used. One of the simplest ways of making the problem determinate would be to have the transmitting aircraft supply its height to the PADAR. The following discussion is based on the assumption that this would be done if the experiment were performed. Neither the analysis nor the results would change much if another technique was used.

Assuming that the transmitter is operating at a known altitude the distance r is now obtained by means of the relation $r = \frac{h'}{\cos\beta}$ instead of by an application of the law of cosines. That is, the situation in the experiment is that which would obtain in Appendix 3 (3.2) if it were assumed that the earth is flat. If we take the limit as $R \to \infty$ in each

equation of that section the resulting equations are precisely those which apply here.

However it will be seen below that if the experiment were performed with the present PADAR equipment, very large errors would generally be found. This is so because the APS-4 antenna of the present PADAR equipment cannot provide angle measurements accurate to better than about three degrees.

One should not rely too heavily on the validity of the Taylor expansion in this case because of the size of the angular errors. Nevertheless, for angles satisfying the restrictions imposed in Appendix 2 (2.5) it will still be valid. The exact error, Equation (3.2.7), may always be examined in any specific case to decide what approximations may be made.

We examine an interesting special case:

Consider the quantity Δr. We measure r by

$$r = \frac{h'}{\cos\beta} .$$

Hence

$$\Delta r = h' \frac{\cos\beta - \cos\beta\cos\Delta\beta + \sin\beta\sin\Delta\beta}{\cos\beta(\cos\beta\cos\Delta\beta - \sin\beta\sin\Delta\beta)} + \frac{\Delta h'}{\cos\beta}$$

or

$$\frac{\Delta r}{r} = \frac{\cos\beta - \cos\beta\cos\Delta\beta + \sin\beta\sin\Delta\beta}{\cos(\beta + \Delta\beta)} + \frac{\Delta h'}{h'} .$$

For the APS-4 receiver, $\Delta\beta \cong 3^\circ \approx .1$ rad. Clearly for β near 90°, $\frac{\Delta r}{r}$ can be infinite. ($\frac{\Delta r}{r} \to \infty$ as $\beta + \Delta\beta \to 90^\circ$). However, this does not necessarily preclude the possibility of obtaining range information. If r is actually much greater than ℓ_1 (and $\phi \neq 0$), the range determination is rather insensitive to r so that one could obtain an accurate value of ℓ_1 in spite of a very large error in r. To determine the expected errors in ℓ_1 in this situation we see that

$$\Delta\ell_1 \xrightarrow[\beta+\Delta\beta \to 90^\circ]{} \frac{\delta^2(2-v)\,\Delta r + 2(vr+\delta)\,\Delta\delta\,\Delta r - \delta(2r+\delta)\,\Delta v\,\Delta r}{2(vr+\delta)(v\Delta r + \Delta v\,\Delta r)}$$

or

$$\Delta\ell_1 \to \frac{\delta^2(2-v) + (2vr+2\delta)\Delta\delta - \delta(2r+\delta)\left[\sqrt{(2-v)v}\,\Delta\phi + \frac{1-v}{2}(\Delta\phi)^2\right]}{2(vr+\delta)\left[v + \sqrt{(2-v)v}\,\Delta\phi + \frac{1-v}{2}(\Delta\phi)^2\right]}$$

$$\frac{\Delta\ell_1}{\ell_1} \to \frac{\frac{\delta(2-v)}{2r+\delta} + 2\frac{(vr+\delta)}{(2r+\delta)}\frac{\Delta\delta}{\delta} - \left[\sqrt{(2-v)v}\,\Delta\phi + \frac{1-v}{2}(\Delta\phi)^2\right]}{v + \sqrt{(2-v)v}\,\Delta\phi + \frac{1-v}{2}(\Delta\phi)^2}$$

NOTE: ϕ is not necessarily small when $\beta = 90^\circ$, since the latter is true when the plane of transmitter, reflector, and receiver is horizontal.

Computations based on the above error equations show that in almost all cases the errors obtained in the experiment would be intolerably large. Because of this and such factors as the non-comparability of the cross-sections and equipment we do not believe that the proposed experiment could give results which would be capable of interpretation in terms of the missile problem.

3.4 Bistatic Radar Systems

The growing complexity of the defense and early-warning problems has led to the adoption of the bistatic method of operation in parts of the defense system. In the light of probable future developments in the decoy field and the advantages of bistatic detection which are discussed in Reference 11, it seems probable that more use will be made of bistatic radar.

It was observed in an investigation made in 1952 that the principle used in PADAR could be made to give range information in a pulsed bistatic system, (Ref. 12). Its use for this purpose was suggested by an article on the ranging of atmospheric irregularities in which the basic idea appeared, (Ref. 13).

One can say without computation that in most cases the accuracy of the range information obtained should be better than that obtained in any of the proposed applications of PADAR. This is so because only one angular measurement is required and that one is made from the ground.

REFERENCES

1. PADAR Investigation, Fairchild Guided Missiles Division, Progress Report 1, 64M-0001, 1955, CONFIDENTIAL.

2. PADAR Investigation, Fairchild Guided Missiles Division, Progress Report 64M-0002, 1955, CONFIDENTIAL.

3. PADAR Investigation, Fairchild Guided Missiles Division, Progress Report 64M-0003, 1955, CONFIDENTIAL.

4. PADAR Investigation, Fairchild Guided Missiles Division, Progress Report 64M-0004, 1956, CONFIDENTIAL.

5. PADAR Investigation, Fairchild Guided Missiles Division, Special Progress Report, Report 64R-5, 1956, CONFIDENTIAL.

6. "Studies in Radar Cross-Sections XV - Radar Cross-Sections of B-47 and B-52 Aircraft", C. E. Schensted, J. W. Crispin, and K. M. Siegel, The University of Michigan, Engineering Research Institute, (2260-1-T, August 1954) AF-33(616)-2531, CONFIDENTIAL.

7. "Propagation of Short Radio Waves", Volume 13, Kerr, D. E., MIT Radiation Laboratory Series, McGraw-Hill Book Company, 1951.

8. "A Study of Electronic Countermeasures for Application Against Air Defense Guided Missile System", The University of Michigan, Engineering Research Institute, UMM-111, April 1953, SECRET.

9. "Talos in the Air Defense of the United States", The Johns Hopkins University, Applied Physics Laboratory, TG 190-2, April 1953, SECRET.

10. "Battlefield Surveillance Radar Systems", The University of Michigan, internal report, January 1956, SECRET.

11. "Studies in Radar Cross-Sections XVIII - Airborne Passive Measures and Countermeasures", K. M. Siegel, M. L. Barasch, J. W. Crispin, R. F. Goodrich, A. H. Halpin, A. L. Maffett, W. C. Orthwein, C. E. Schensted, and C. J. Titus, The University of Michigan, Engineering Research Institute, (2260-29-F, January 1956) AF-33(616)-2531, SECRET.

12. "An Examination of Bistatic Early Warning Radars", K. M. Siegel, The University of Michigan, Engineering Research Institute, (UMM-98, August 1952) W-33(038)-ac-15222, SECRET.

13. "A Forward Transmission Echo Ranging System", D. B. Harris, Proceedings of the Institute of Radio Engineers, 37, 767-770 (1949), UNCLASSIFIED.